Supplementary material for the *Observation-based evaluation of the Destination Earth climate change adaptation digital twin simulations using OBSALL v1.0*

Heikki Järvinen[1], Jouni Räisänen[1], Lauri Tuppi[1], Clement Bouvier[1], Antonio Sanchez-Benitez[2], Juniper Tyree[1], Antti Toropainen[1], Paolo Davini[4], Francisco Doblas-Reyes[6], Thomas Jung[2,3], Daniel Klocke[7], Jenni Kontkanen[8], Sebastian Milinski[9], Matteo Nurisso[5], Himansu Kesari Pradhan[2], Irina Sandu[9]

[1]Institute for Atmospheric and Earth System Research (INAR), University of Helsinki, Helsinki, Finland
[2]Alfred-Wegener-Institut, Helmholtz-Zentrum für Polar- und Meeresforschung (AWI), Bremerhaven, Germany
[3]Institute of Environmental Physics, University of Bremen, Bremen, Germany
[4]Consiglio Nazionale delle Ricerche, Istituto di Scienze dell'Atmosfera e del Clima (CNR-ISAC), Torino, Italy
[5]Department of Environment, Land and Infrastructure Engineering, Politecnico di Torino, Torino, Italy
[6]Barcelona Supercomputing Center (BSC), Barcelona, Spain
[7]Max-Planck-Institut für Meteorologie (MPI-M), Hamburg, Germany
[8]CSC – IT Center for Science, Espoo, Finland
[9]European Centre for Medium-Range Weather Forecasts (ECMWF), Bonn, Germany

Correspondence to: Heikki Järvinen (heikki.j.jarvinen@helsinki.fi)

Contents

This supplement includes a catalogue of forty Figures from the evaluation of the model simulations against synoptic station observations. There are two Figures for each variable (2-metre temperature (T2), 2-metre dew point difference (DPD2), 10-metre wind speed (V10)) and each statistic, one showing annual cycles of monthly mean values at the three stations studied in the main manuscript (Sodankylä, Prague, and Zaragoza), and the other one displaying the annual mean model-minus-observation differences for IFS-NEMO, IFS-FESOM, and ICON. The corresponding Figure numbers are listed in Table S1. The Figures of annual cycles have odd (S1, S3 ... S13 and S17, S19 ... S39) and the maps even Figure numbers (S2, S4, ... S14 and S18, S20 ... S40). In addition, there are two Figures (S15-16) for heatwave and coldwave statistics.

Table S1. List of supplementary figures. T2 = 2-metre temperature, DPD2 = 2-metre dew point difference, 10-metre wind speed = V10, SD = standard deviation.

	Mean values	Diurnal range	Trends	Interannual SD	Intramonth SD	Return values	Heatwaves Coldwaves
T2	S1-S2	S3-S4	S5-S6	S7-S8	S9-S10	S11-14	S15-16
DPD2	S17-S18	S19-S20	S21-S22	S23-S24	S25-S26	S27-28	
V10	S29-30	S31-32	S33-34	S35-36	S37-S38	S39-40	

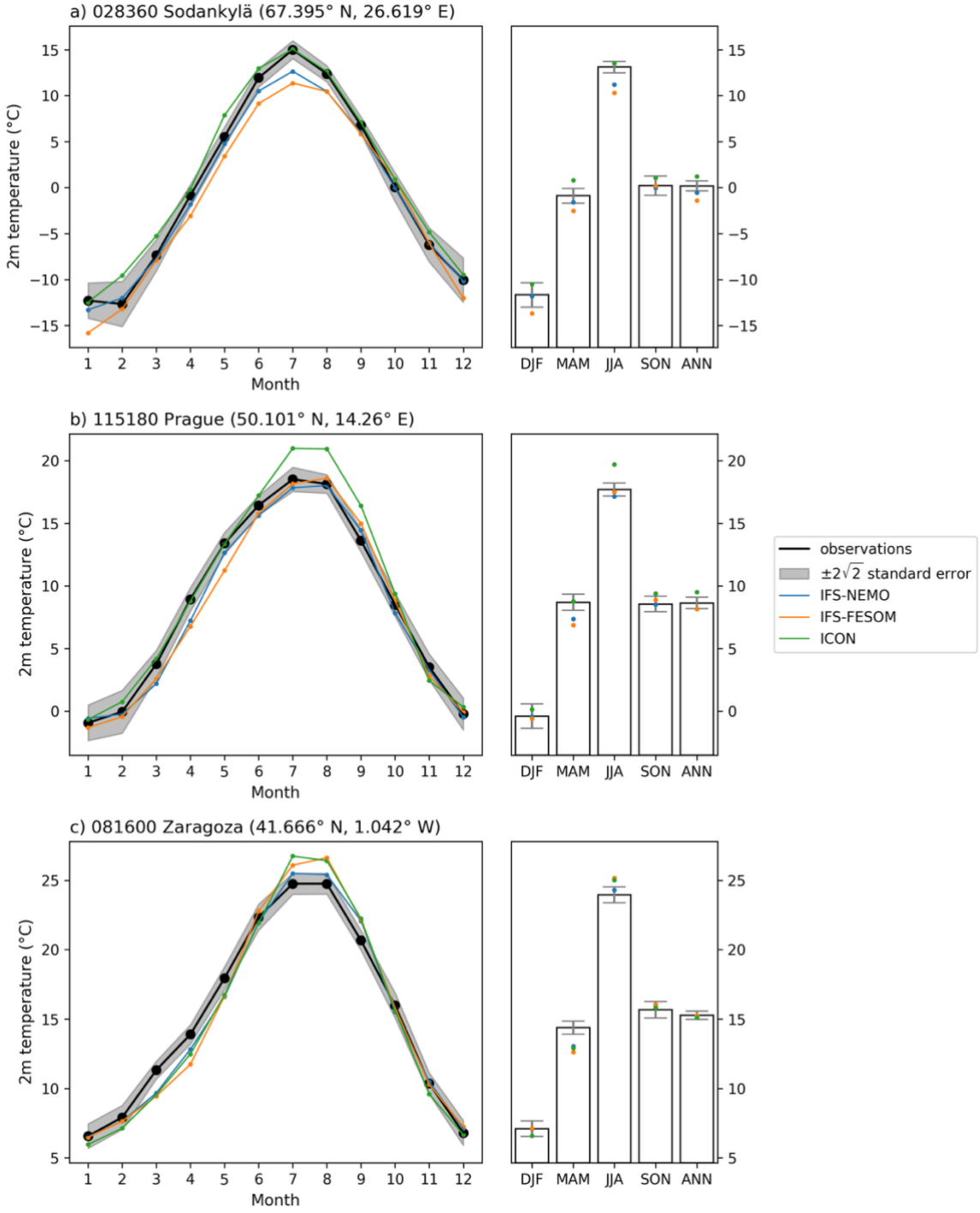

Figure S1. Left: monthly mean values of 2-metre temperature (°C); stations 028360 Sodankylä (top), 115810 Prague (middle), and 081600 Zaragoza (bottom); observations (black), simulations (coloured lines, see the legend). Right: seasonal and annual mean values in observations (bars) and simulations (coloured circles). Shading on the left and error bars on the right cover $\pm 2\sqrt{2}$ standard errors around the observed value.

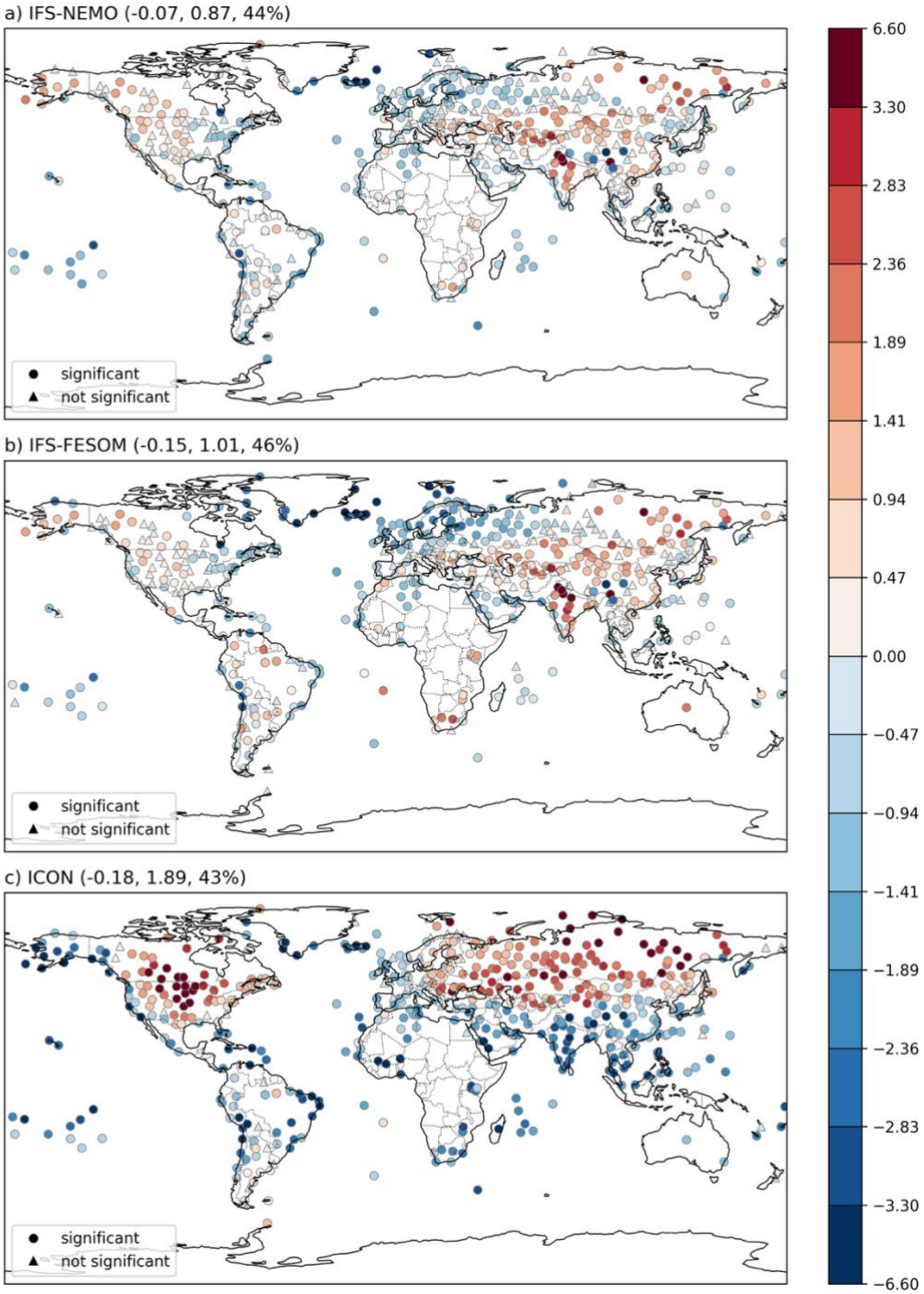

Figure S2. Bias of annual mean 2-metre temperature (°C) in (a) IFS-NEMO, (b) IFS-FESOM and (c) ICON. Stations, where the simulated values differ by more (less) than $\pm 2\sqrt{2}$ standard errors from the observations are marked with closed circles (triangles). The first two numeric values in the headings give the average bias and the average absolute bias over all stations, and the last number reports the percent fraction of stations with positive bias.

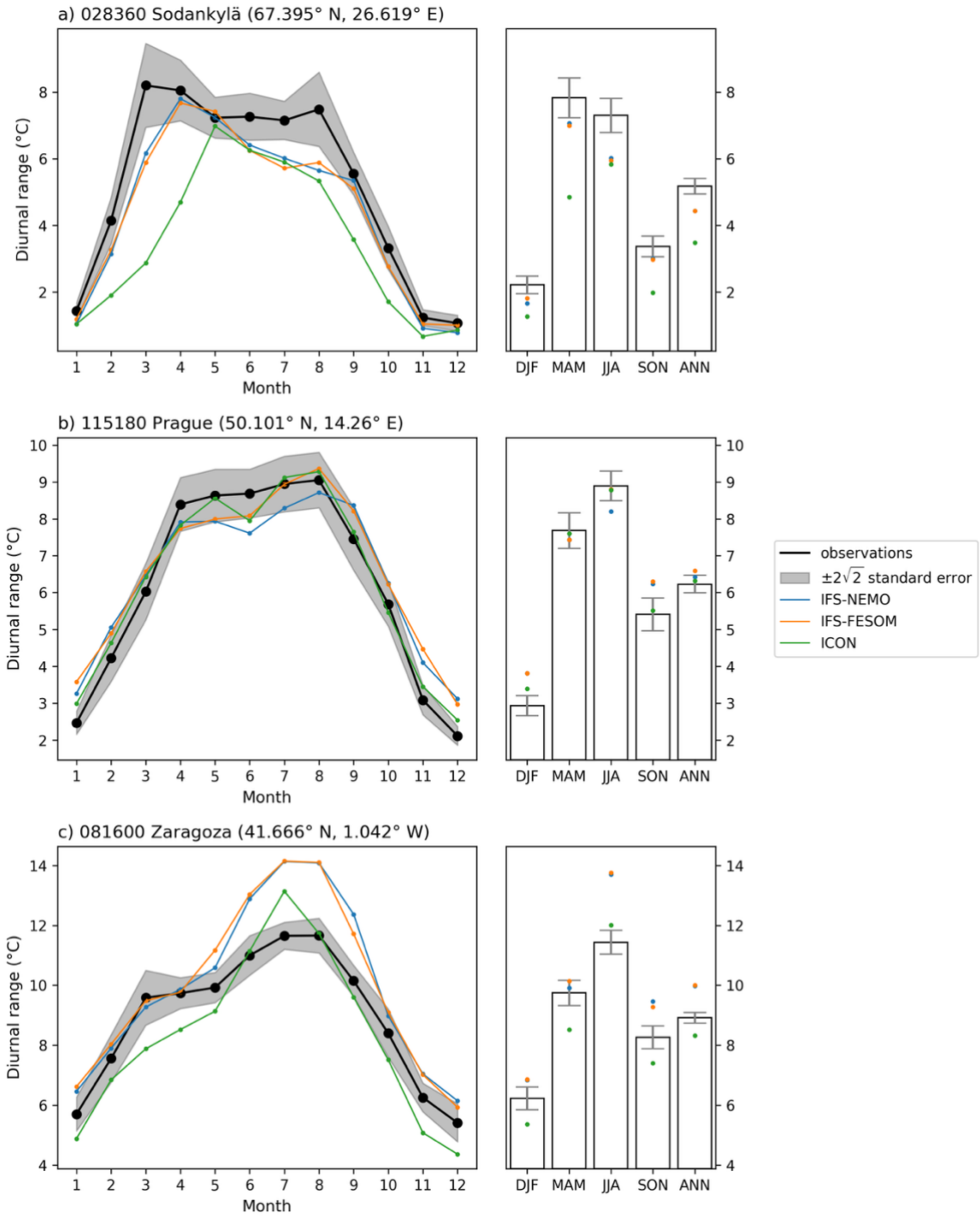

Figure S3. As Figure S1, but for the diurnal range of 2-metre temperature (°C).

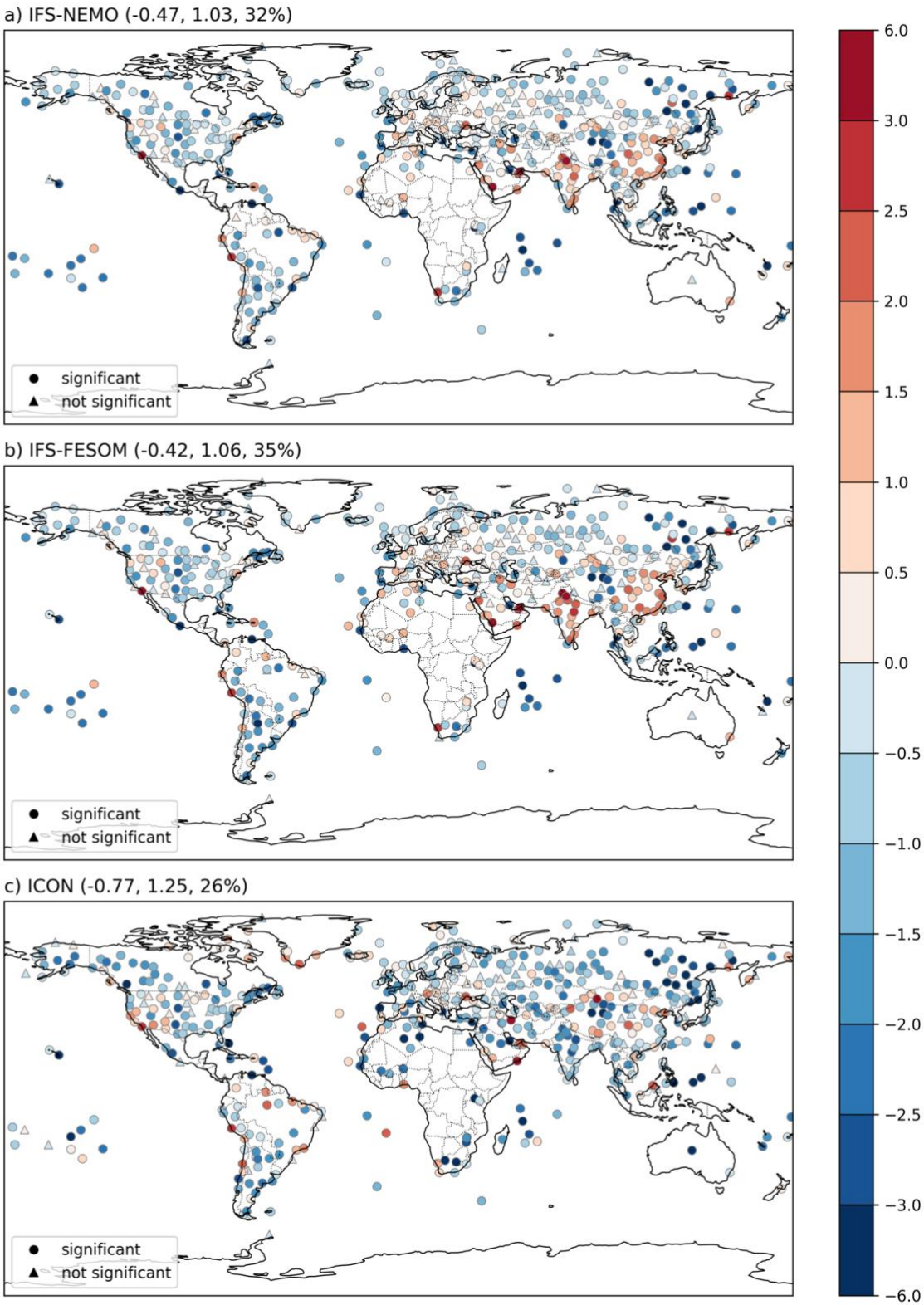

Figure S4. As Figure S2, but for the diurnal range of 2-metre temperature (°C).

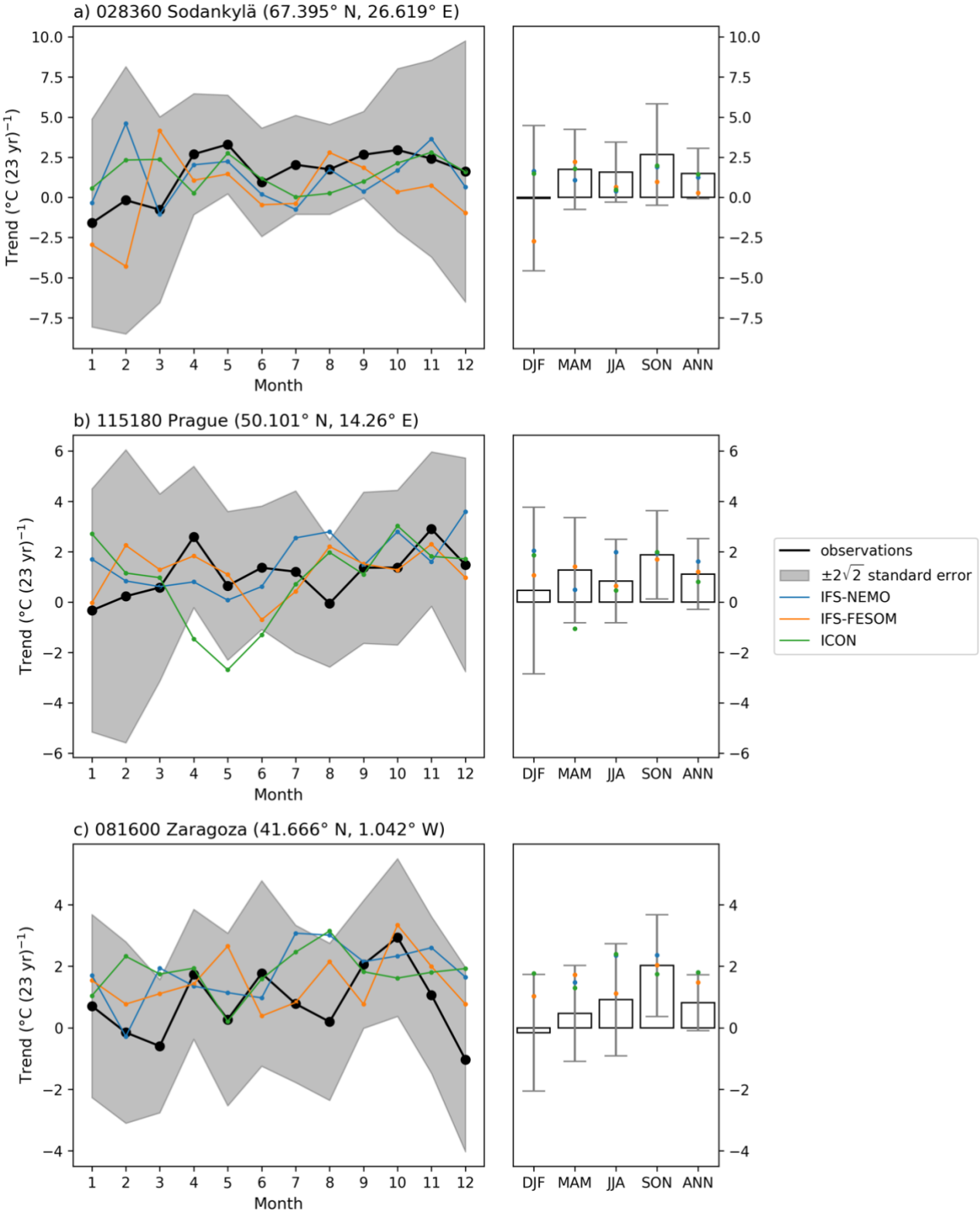

Figure S5. As Figure S1, but for the linear trend of 2-metre temperature (°C (23 yr)$^{-1}$).

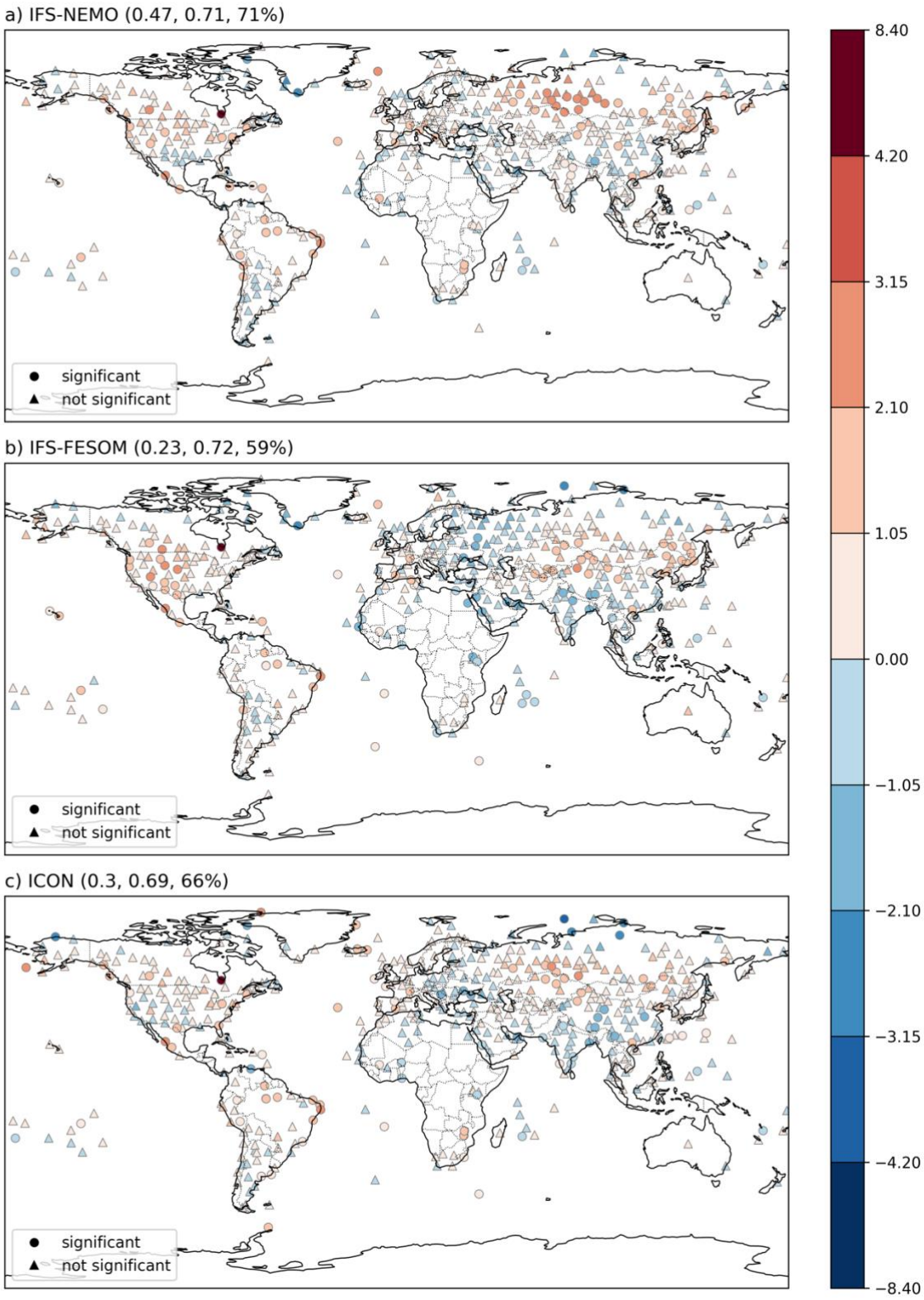

45 **Figure S6**. As Figure S2, but for the linear trend of 2-metre temperature (°C (23 yr)$^{-1}$).

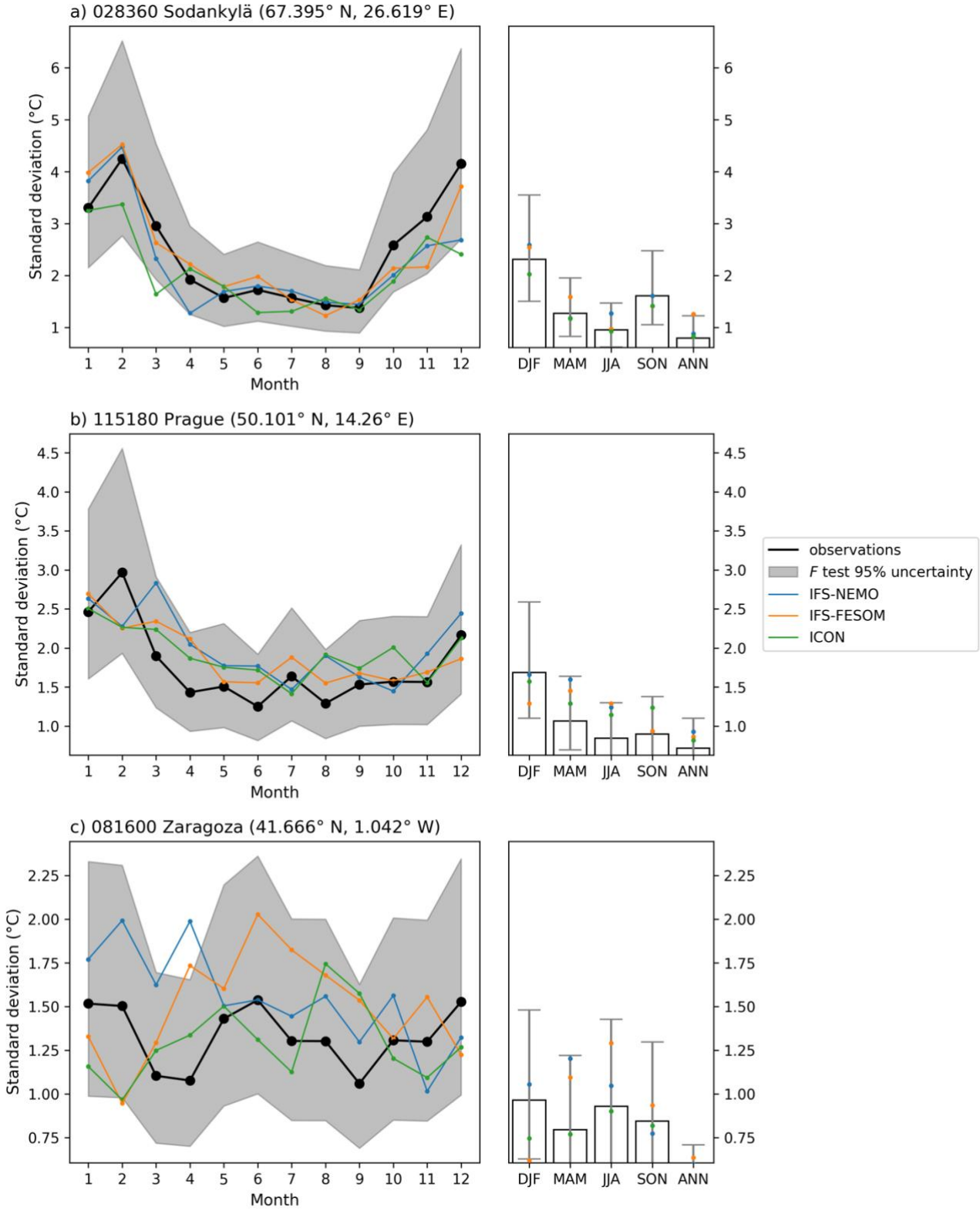

Figure S7. Left: seasonal cycles of interannual standard deviation of 2-metre temperature (°C) at stations 028360 Sodankylä (top), 115810 Prague (middle) and 081600 Zaragoza (bottom) from observations (black) and model simulations (coloured lines, see the legend). Right: interannual standard deviation of seasonal and annual means of 2-metre temperature from observations (bars) and in the simulations (coloured closed circles). Simulated values that fall outside the shading on the left and the error bars on the right differ significantly (5 % risk level in two-sided F-test) from the observed value.

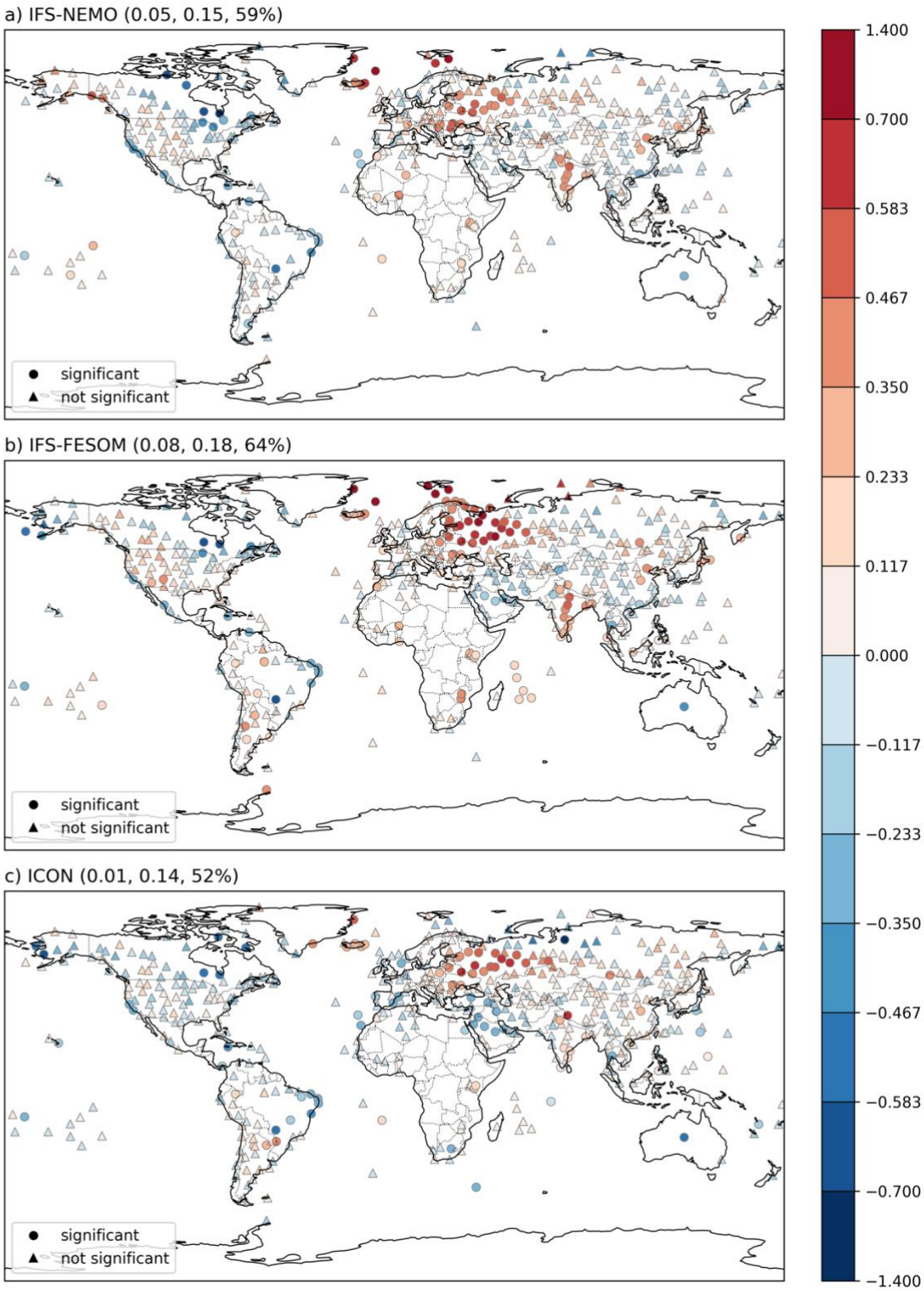

Figure S8. *Model-minus-observation differences of interannual standard deviation of annual mean 2-metre temperature (°C) in (a) IFS-NEMO, (b) IFS-FESOM, and (c) ICON. Stations where the simulated standard deviation differs significantly (5 % risk level in two-sided F-test) from the observed standard deviation are marked with closed circles, and the stations with no significant difference are marked with triangles. The first two numeric values in the headings give the average bias and the average absolute bias over all stations, and the last number reports the percent fraction of stations with positive bias.*

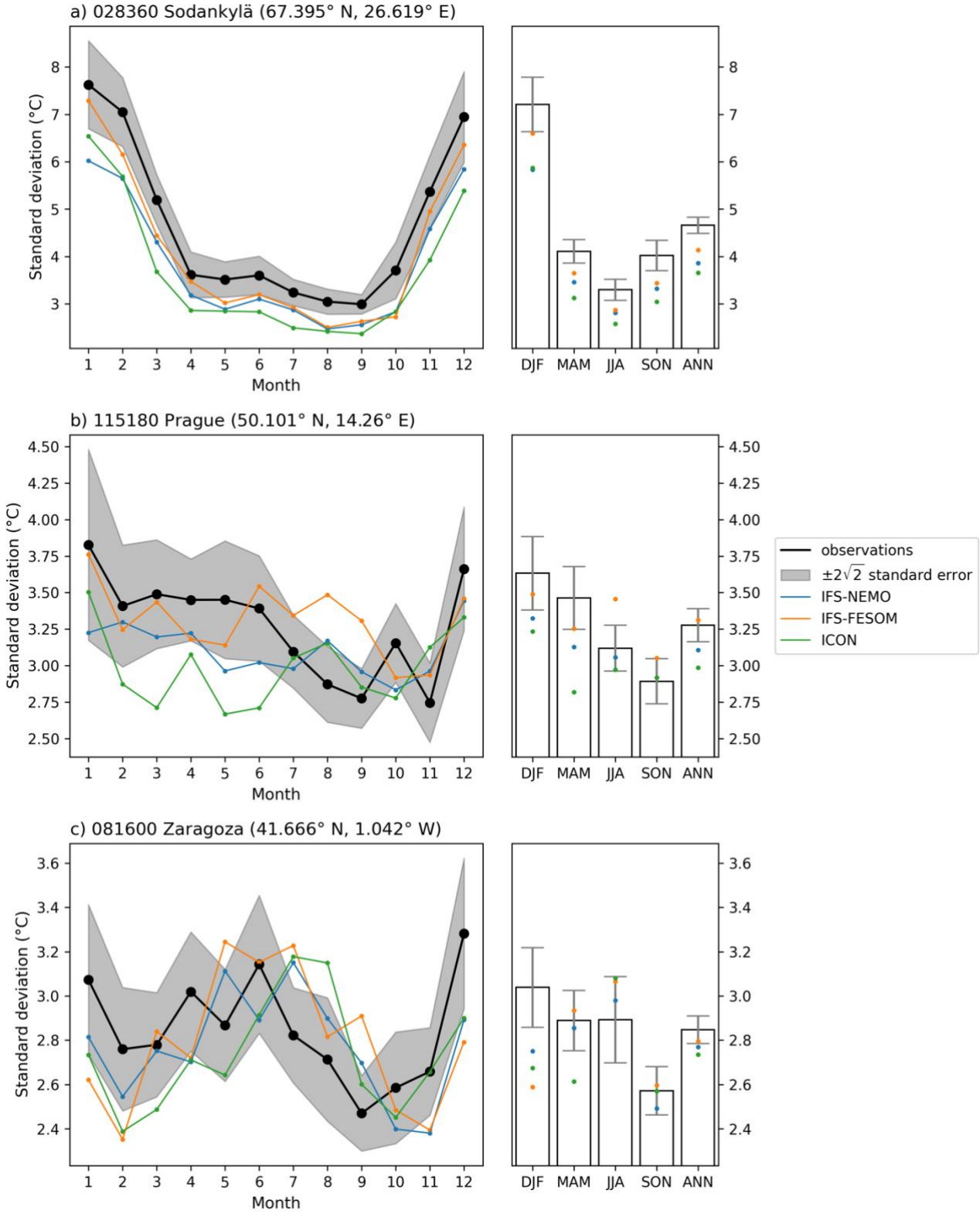

60 **Figure S9**. As Figure S1, but for the intramonth standard deviation of 2-metre temperature (°C).

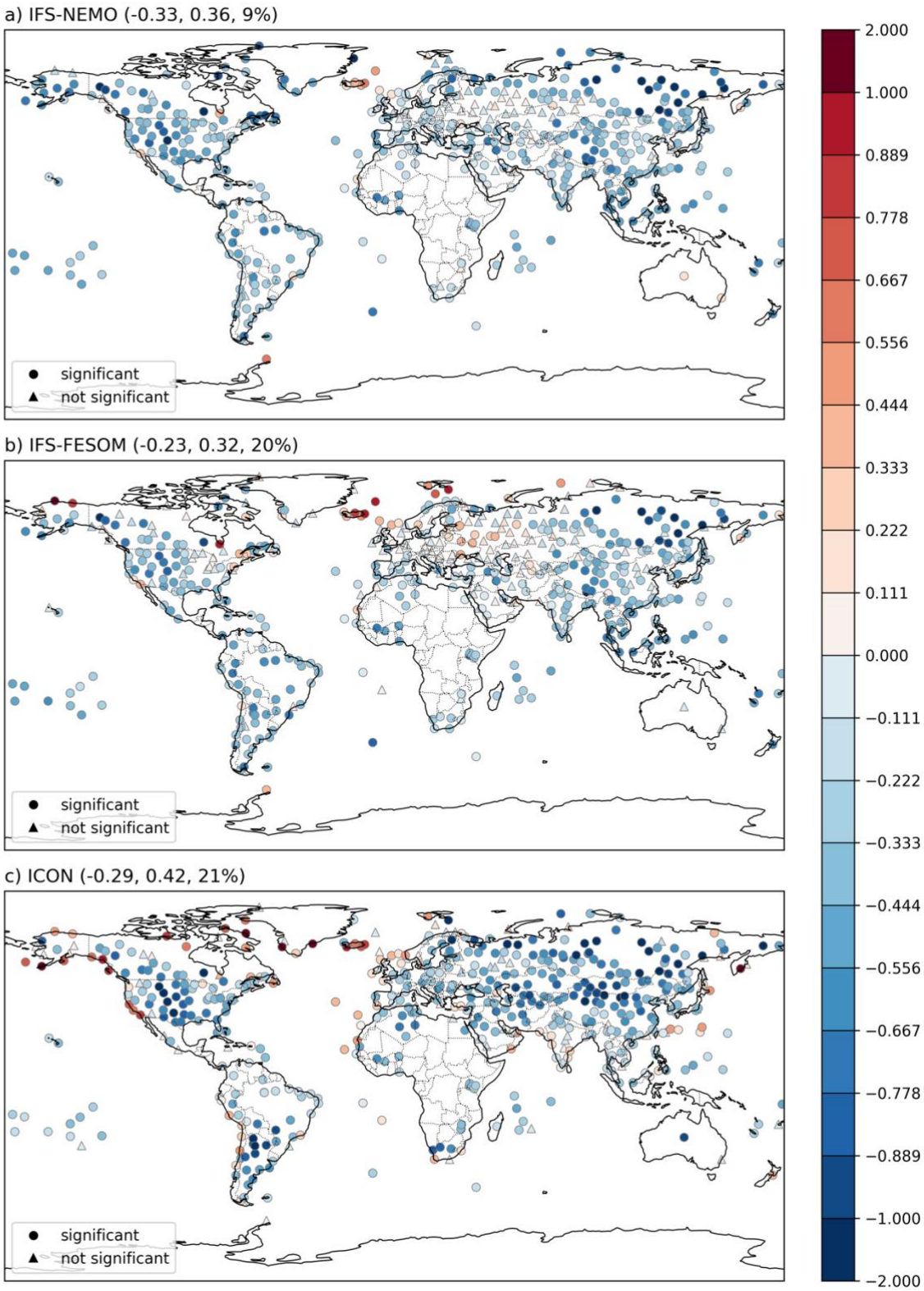

Figure S10. As Figure S2, but for the annually averaged intramonth standard deviation of 2-metre temperature (°C).

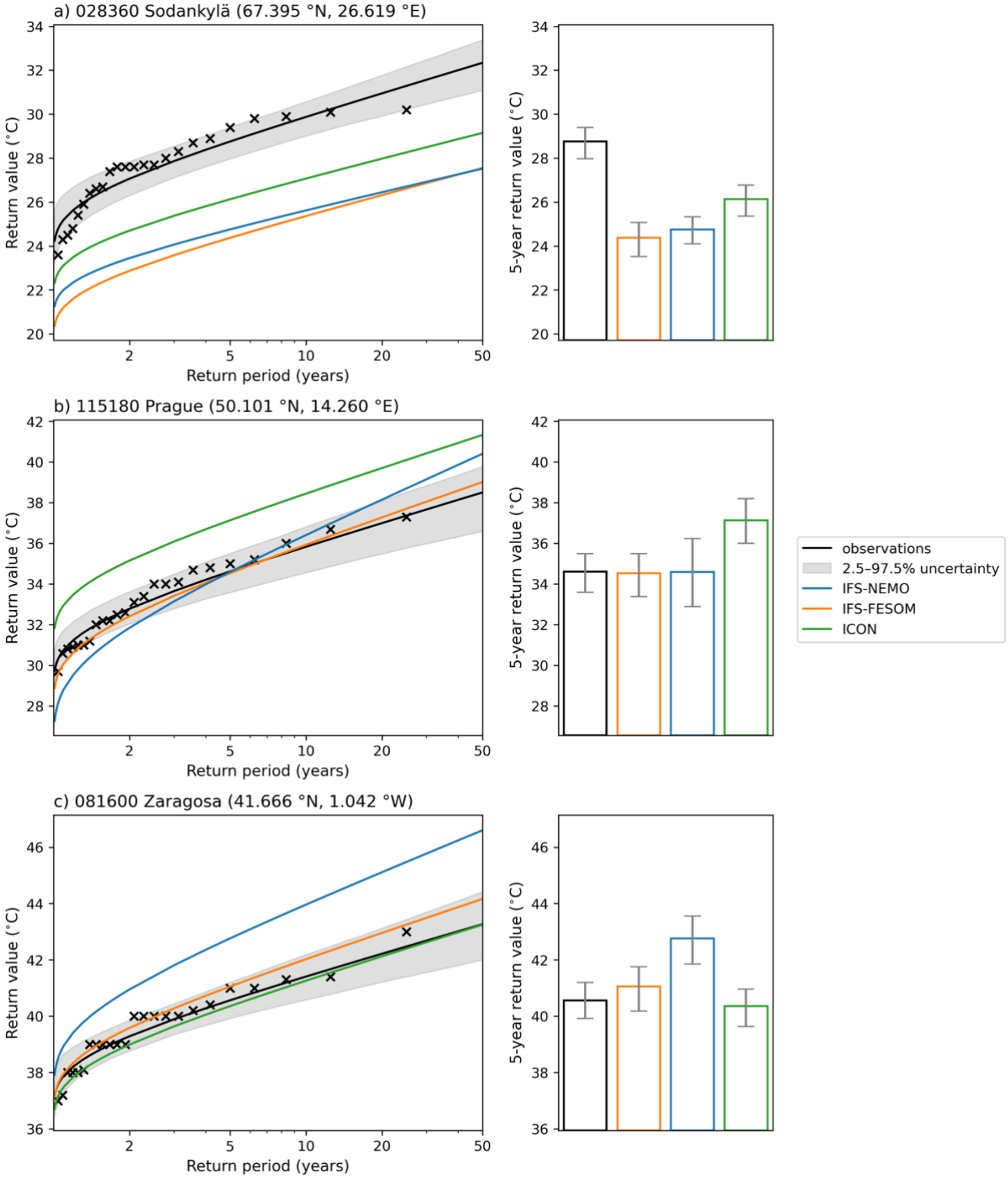

Figure S11. Return values of the highest annual maximum 2-metre temperature (°C) at stations 028360 Sodankylä (top), 115810 Prague (middle) and 081600 Zaragoza (bottom) as a function of return period, based on a Gumbel distribution fit (black - observations; coloured lines – simulations). The shading shows the 2.5-97.5 % uncertainty range of the observed return values based on 1000 bootstrap samples, and the crosses are the observed annual maximum and minimum values in increasing order of extremity. Right: observed (black bars) and simulated (coloured bars) 5-year return values and their 2.5-97.5 % uncertainty ranges (error bars).

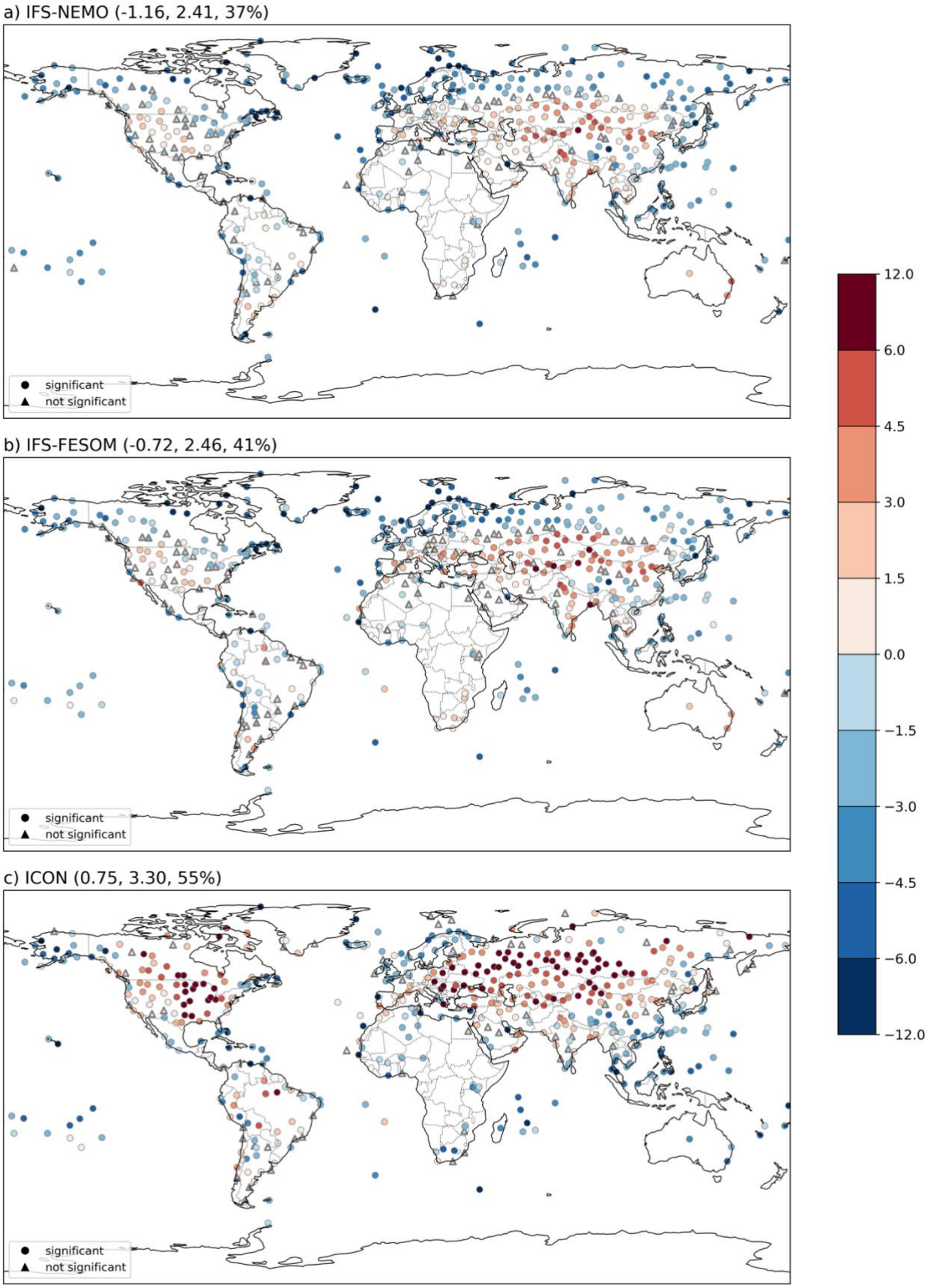

Figure S12. Model-minus-observation differences of the 5-year return values of the highest annual maximum 2-metre temperature (°C) in (a) IFS-NEMO, (b) IFS-FESOM, and (c) ICON. Stations where the simulated return value is outside (inside) the 2.5-97.5% uncertainty range for observations are marked with closed circles (triangles). The first two numeric values in the headings give the average bias and the average absolute bias over all stations, and the last number reports the percent fraction of stations with positive bias.

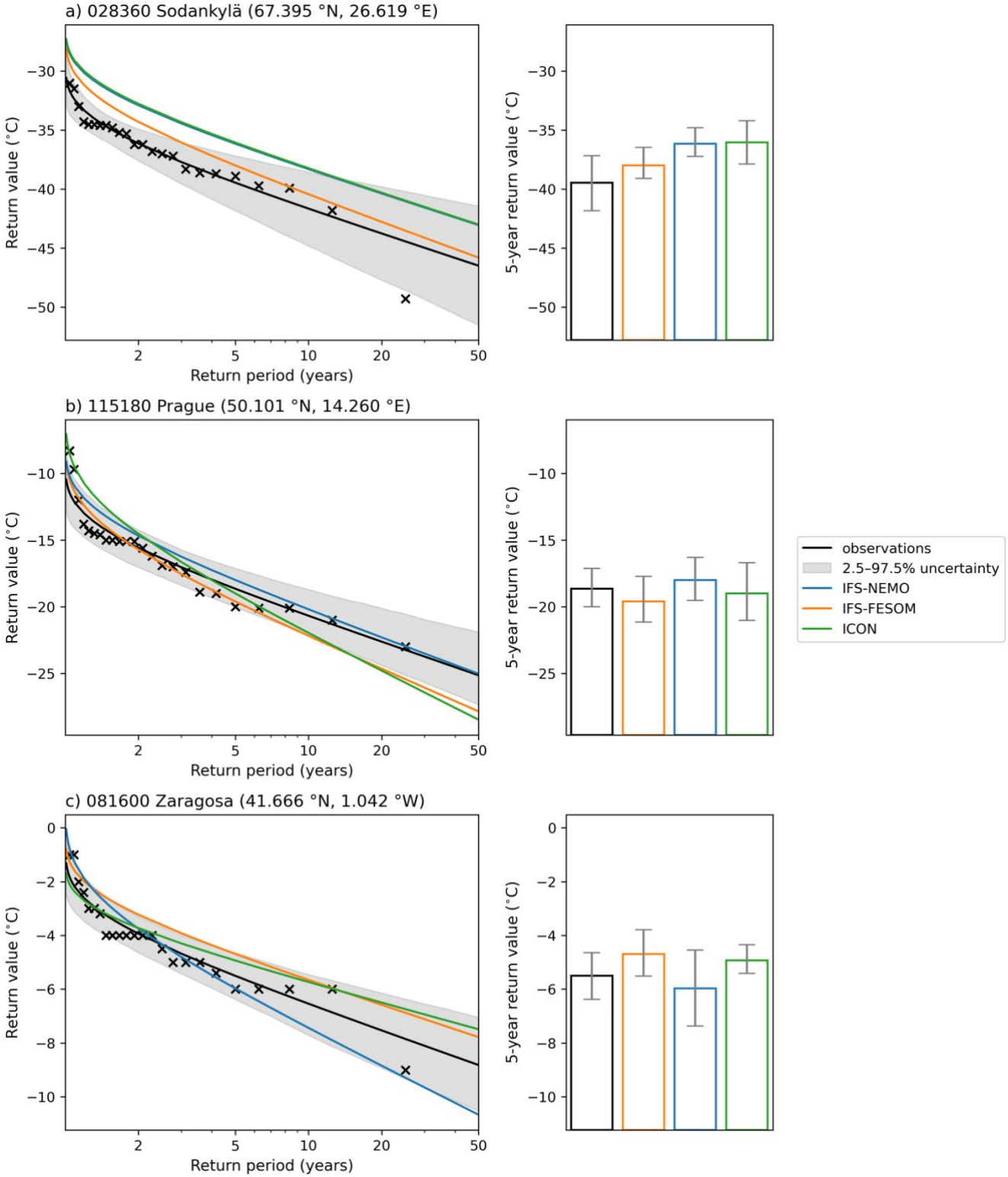

Figure S13. As Figure S11, but for the 5-year return values of the lowest annual minimum 2-metre temperature (°C).

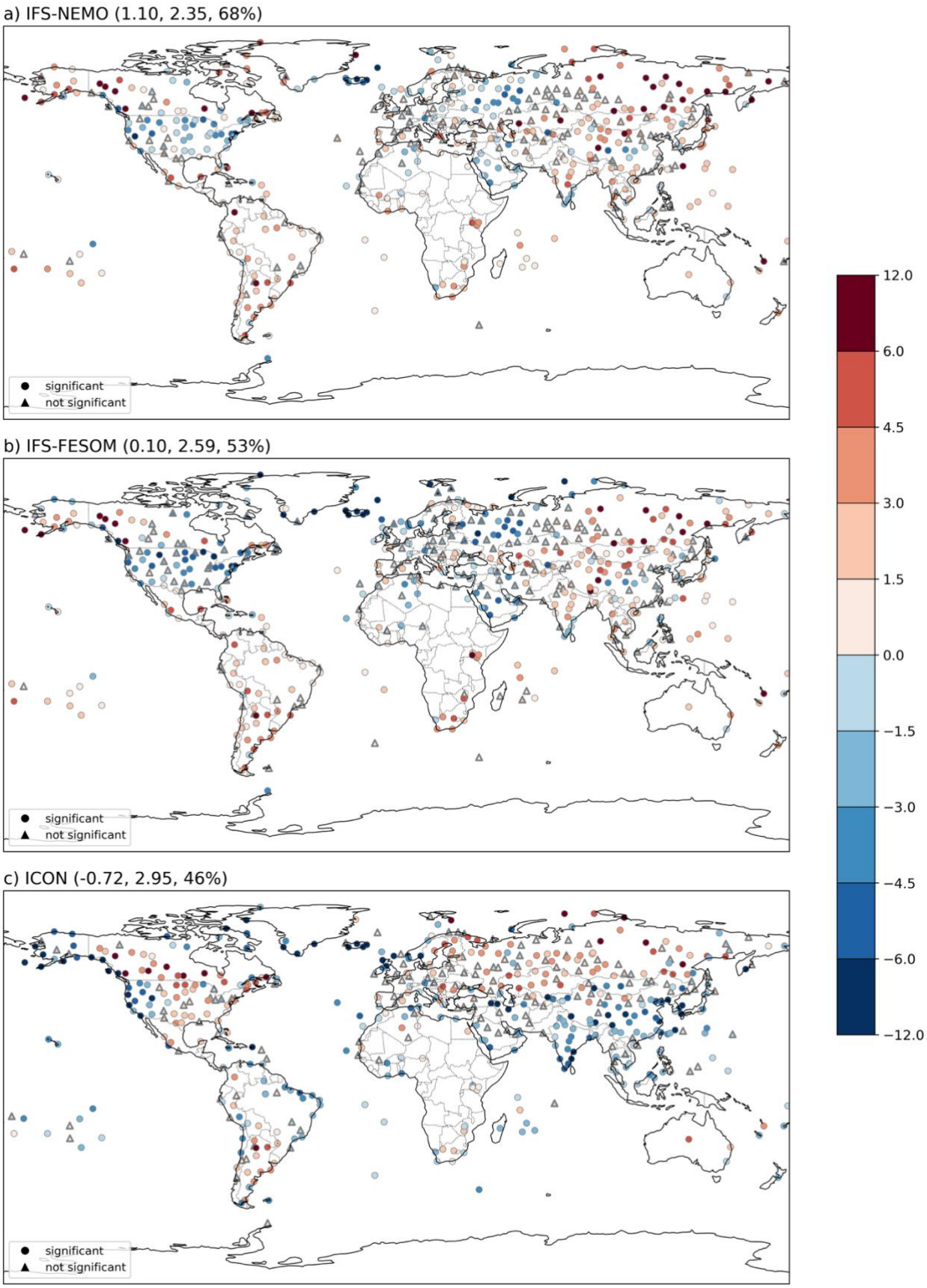

Figure S14. As Figure S12, but for the 5-year return values of the lowest annual minimum 2-metre temperature (°C).

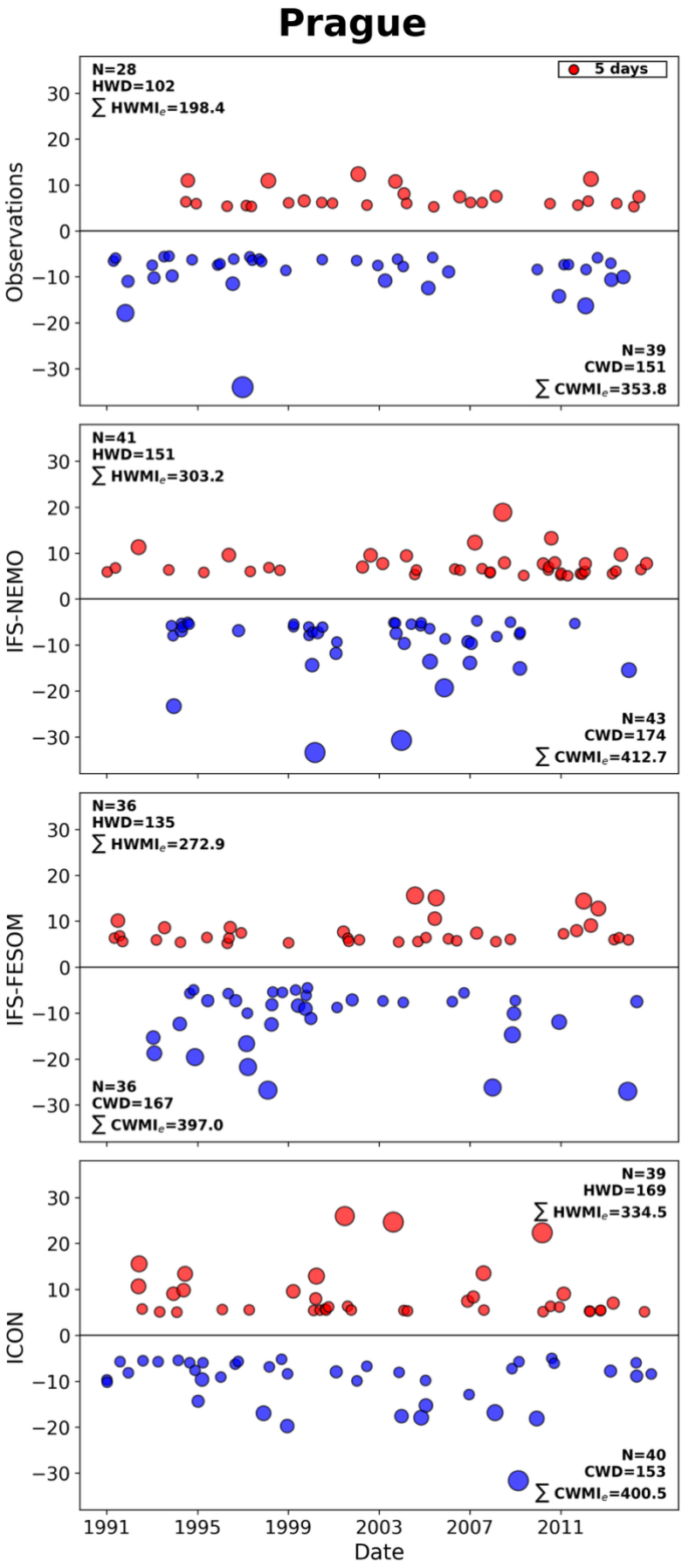

Figure S15. Heatwaves and coldwaves at the station 115180 Prague (the Czech Republic), based on 2-metre temperature observations (top row) and historical simulations from IFS-NEMO (second row), IFS-FESOM (third row), and ICON (fourth row). Red points represent heatwaves ($HWMI_e$), and blue points coldwaves ($CWMI_e$), scaled by –1 for visual symmetry. Point size indicates event duration. In each panel, the top (bottom) portion summarizes heatwave (coldwave) metrics: number of events (N), total number of days (HWD, CWD), and accumulated magnitude indices (Σ $HWMI_e$, Σ $CWMI_e$).

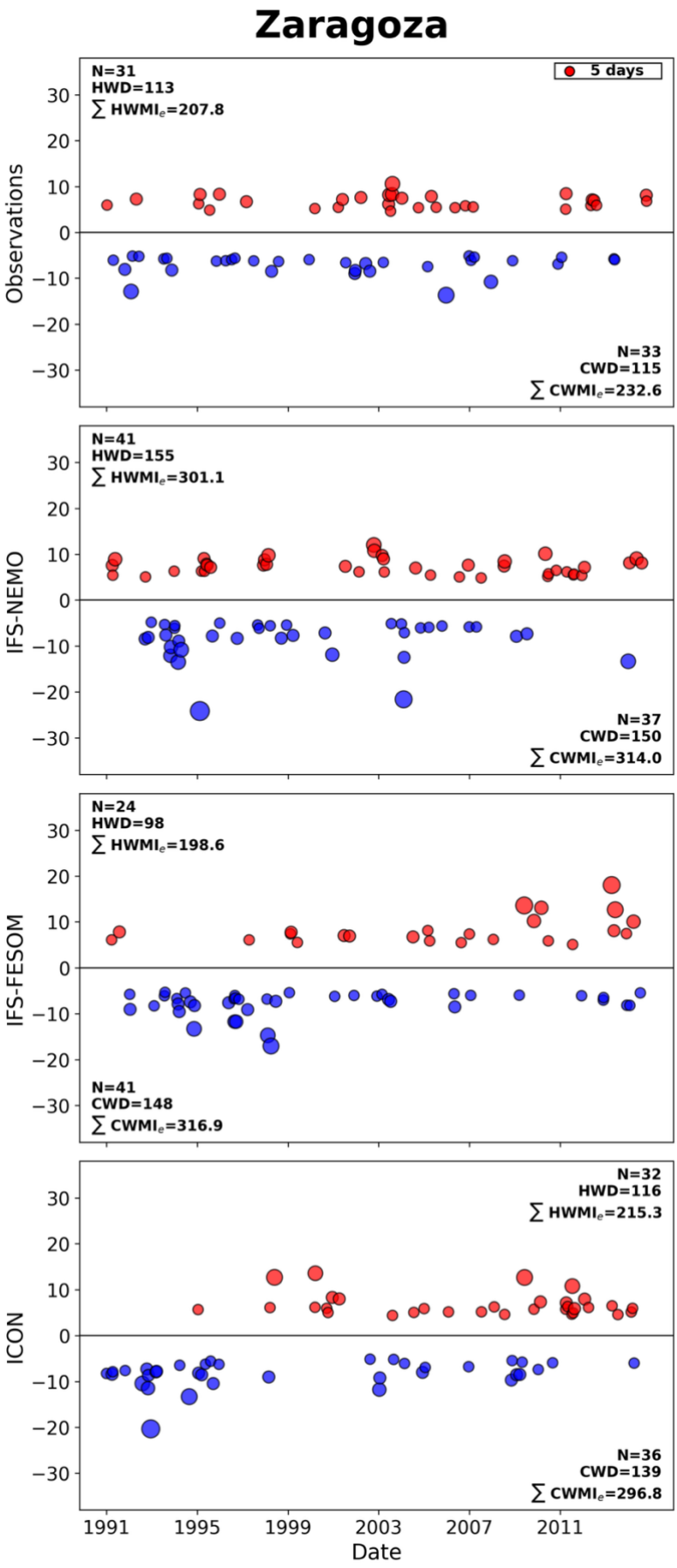

Figure S16. As Figure S15, but for the station 081600 Zaragoza (Spain).

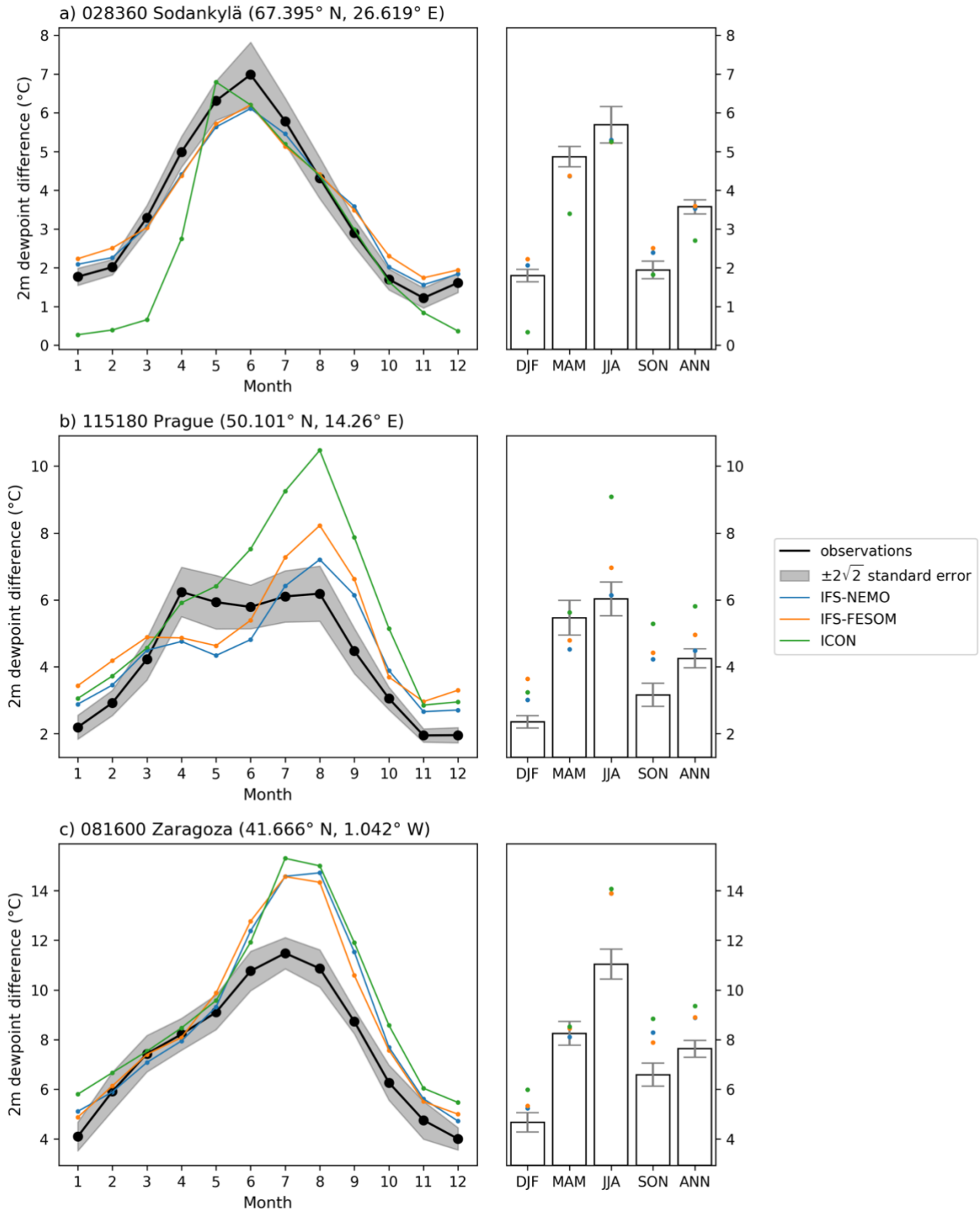

Figure S17. As Figure S1, but for the mean values of 2-metre dew point difference (°C).

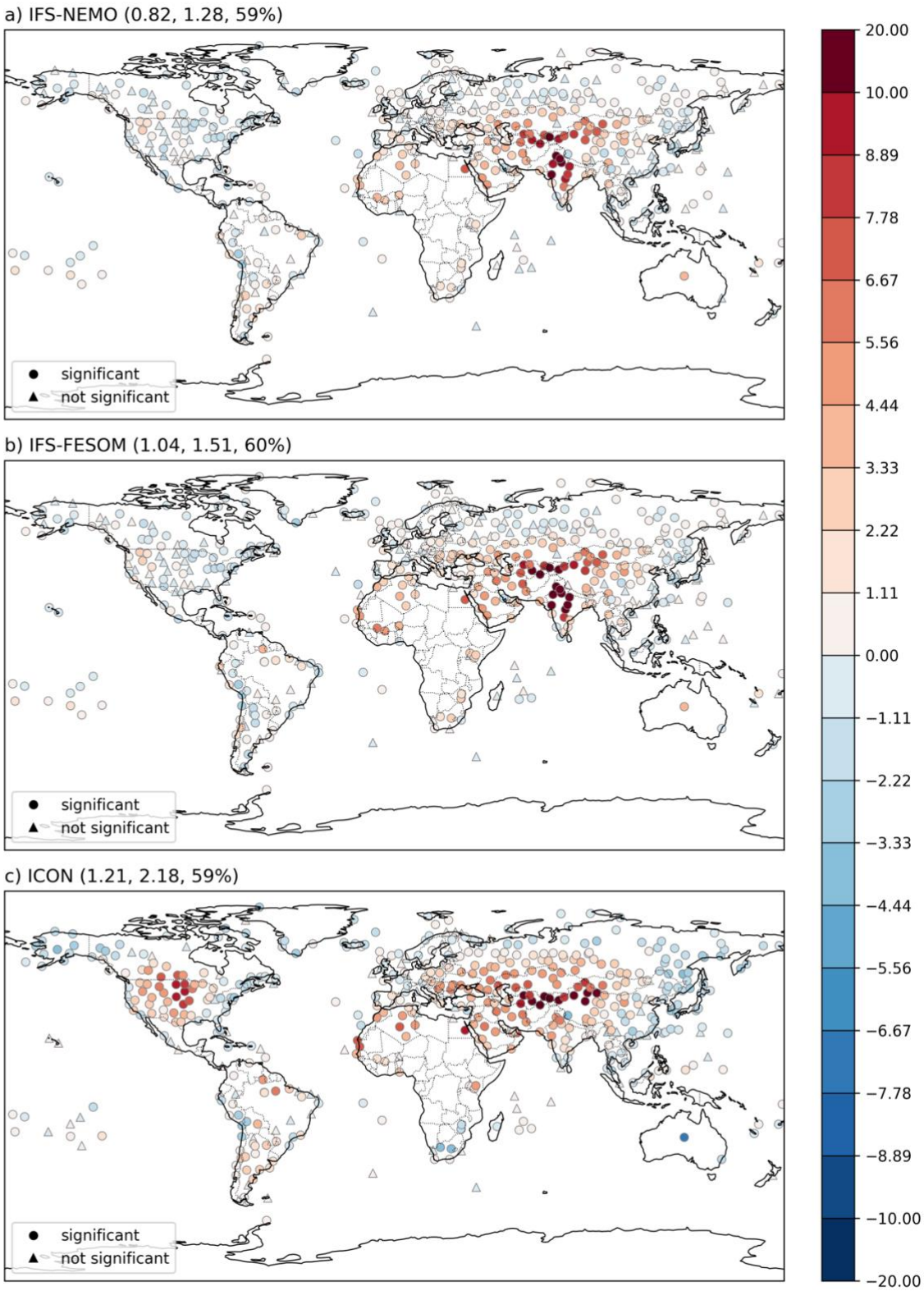

Figure S18. As Figure S2, but for the annual mean 2-metre dew point difference (°C).

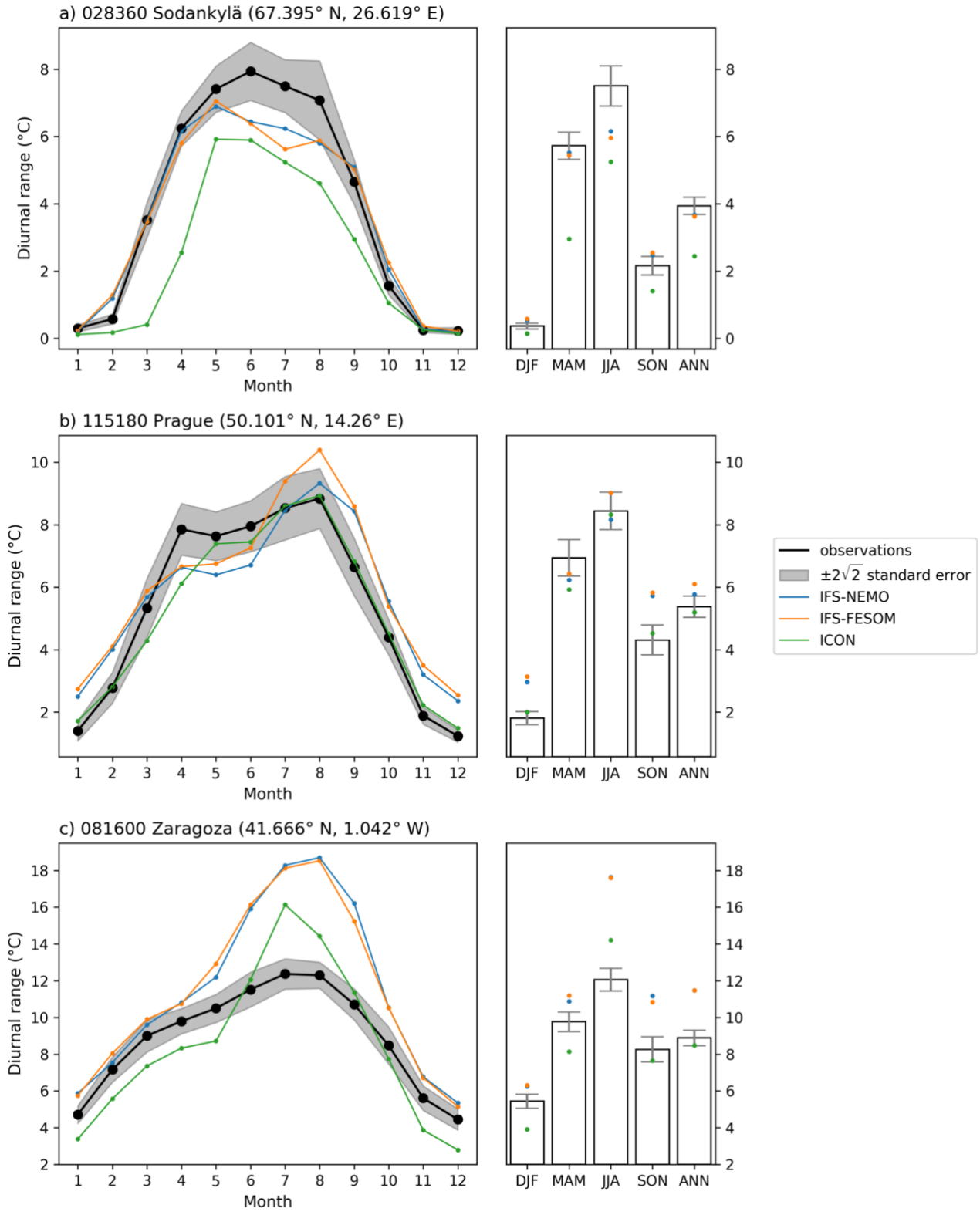

Figure S19. As Figure S3, but for the diurnal range of 2-metre dew point difference (°C).

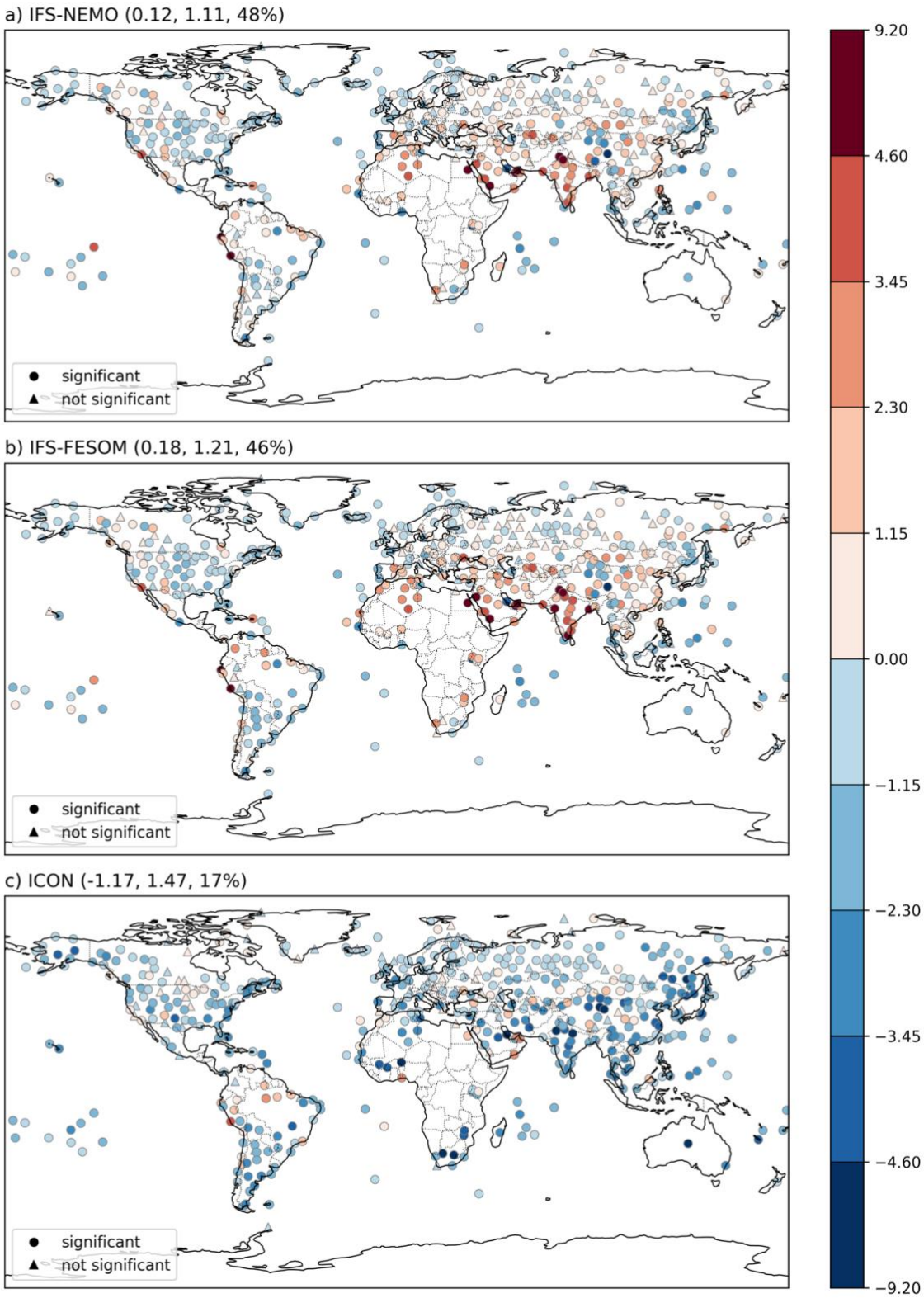

95 **Figure S20**. As Figure S4, but for the diurnal range of 2-metre dew point difference (°C).

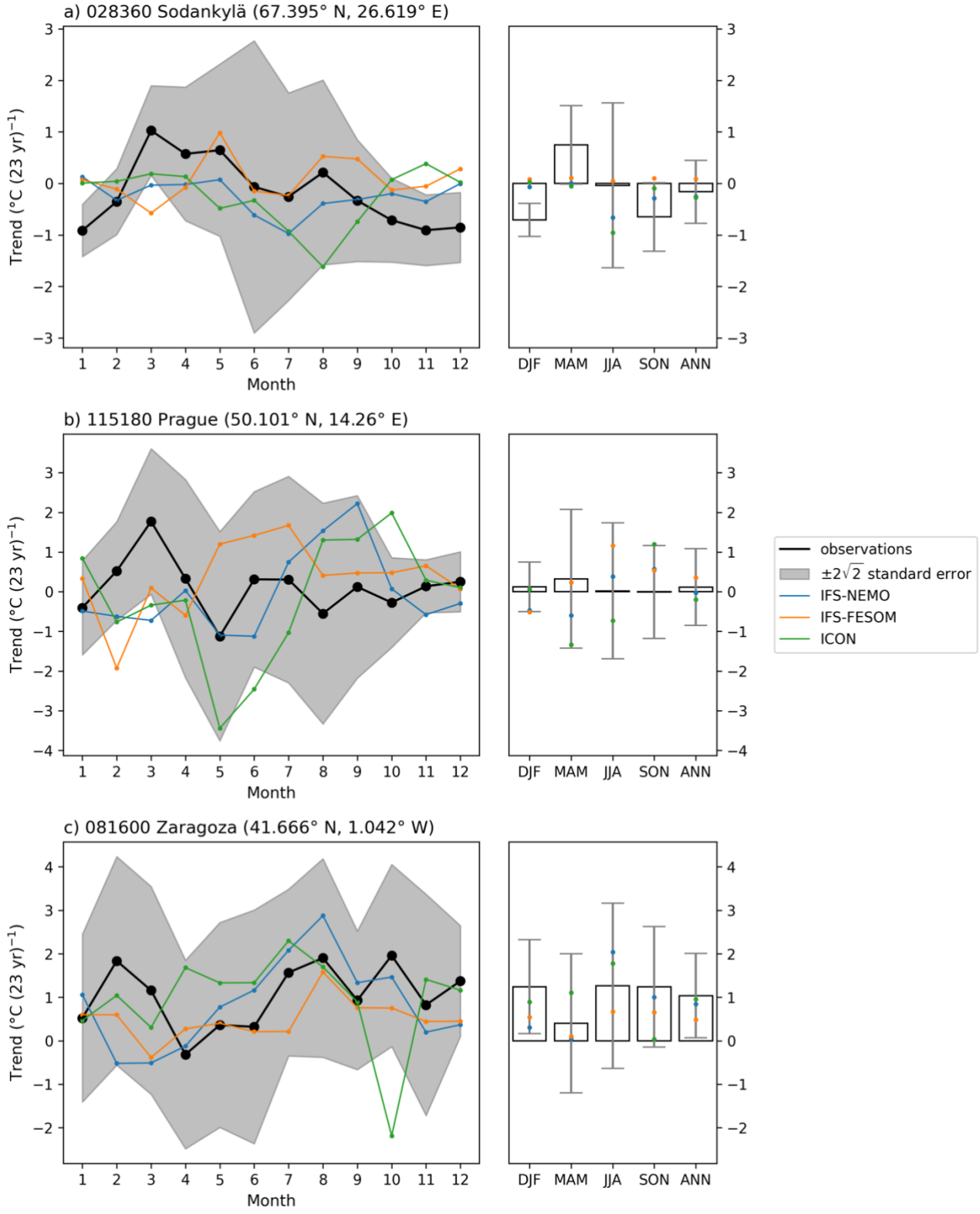

Figure S21. As Figure S5, but for the trend of 2-metre dew point difference (°C (23 yr)$^{-1}$).

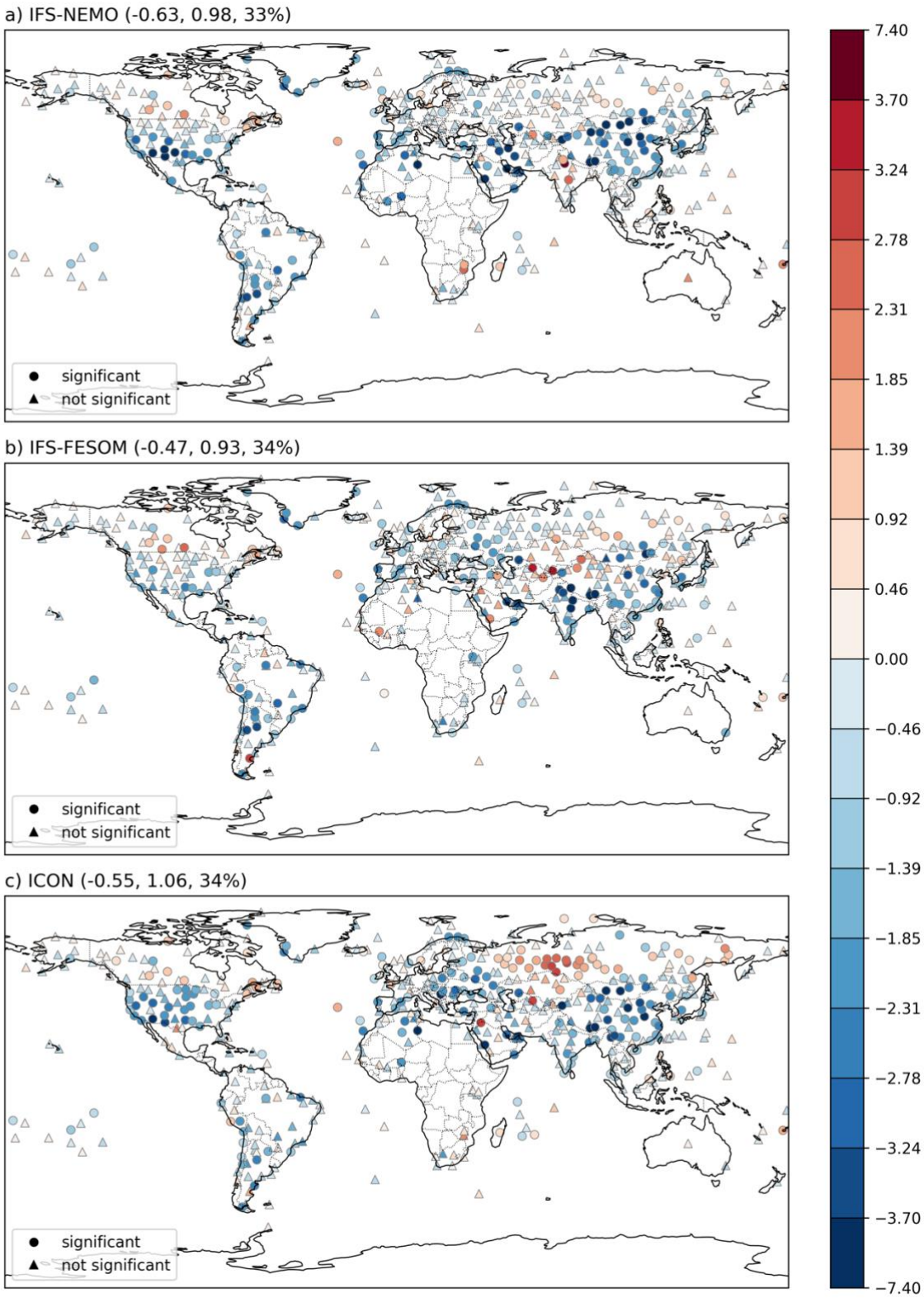

Figure S22. As Figure S6, but for the trend of annually averaged 2-metre dew point difference (°C (23 yr)$^{-1}$).

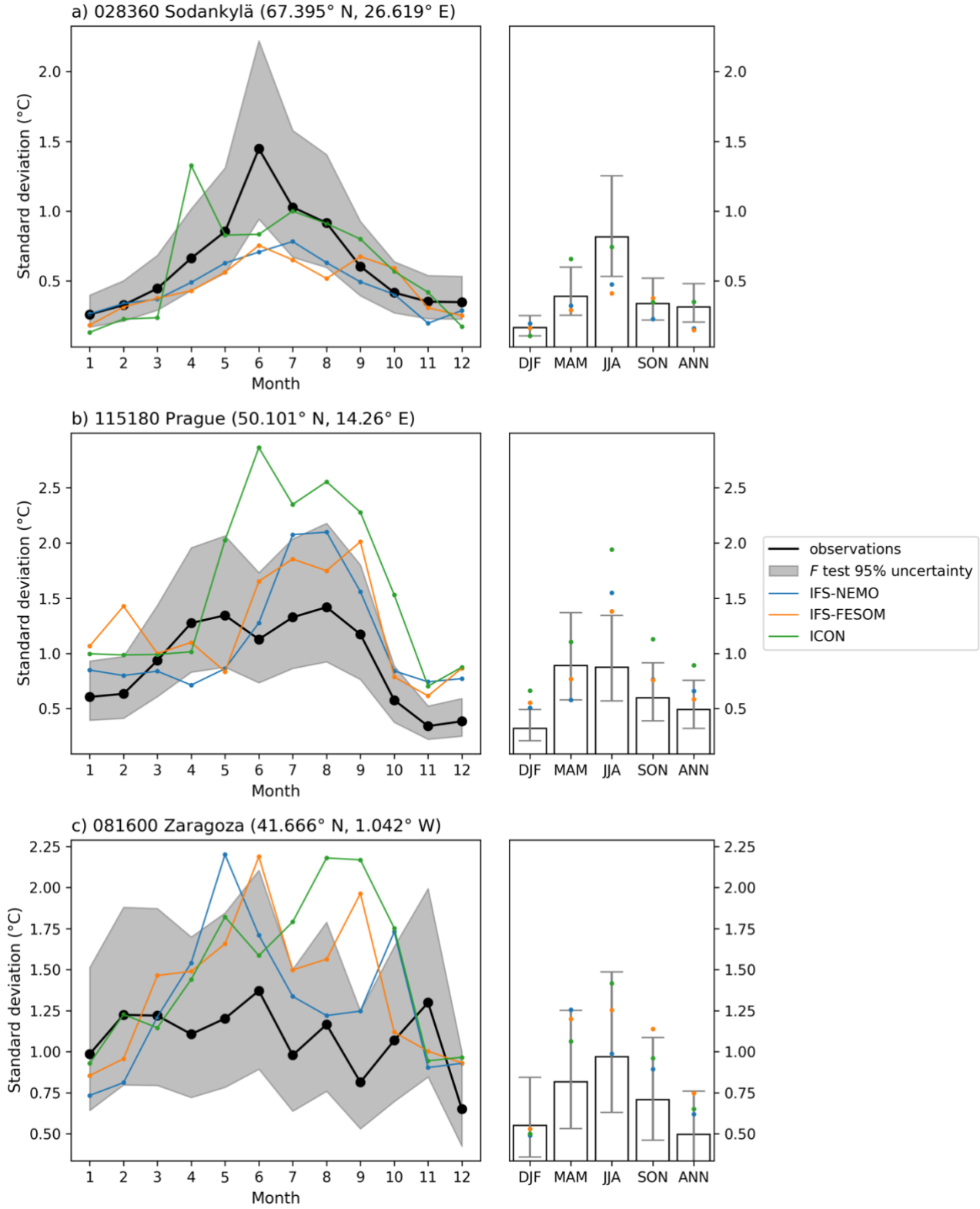

100

Figure S23. As Figure S7, but for the interannual standard deviation of 2-metre dew point difference (°C).

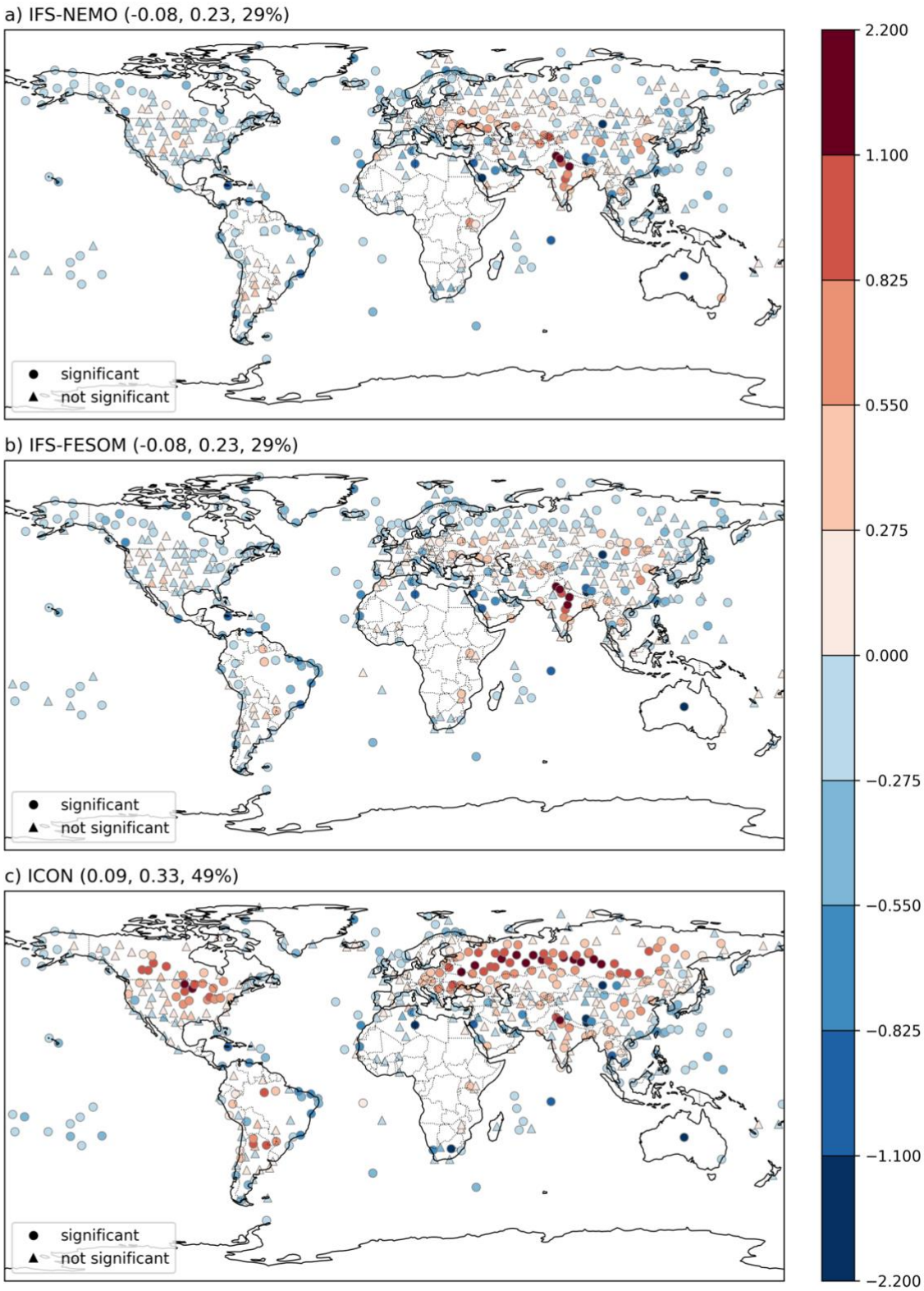

Figure S24. As Figure S8, but for the interannual standard deviation of annually averaged 2-metre dew point difference (°C).

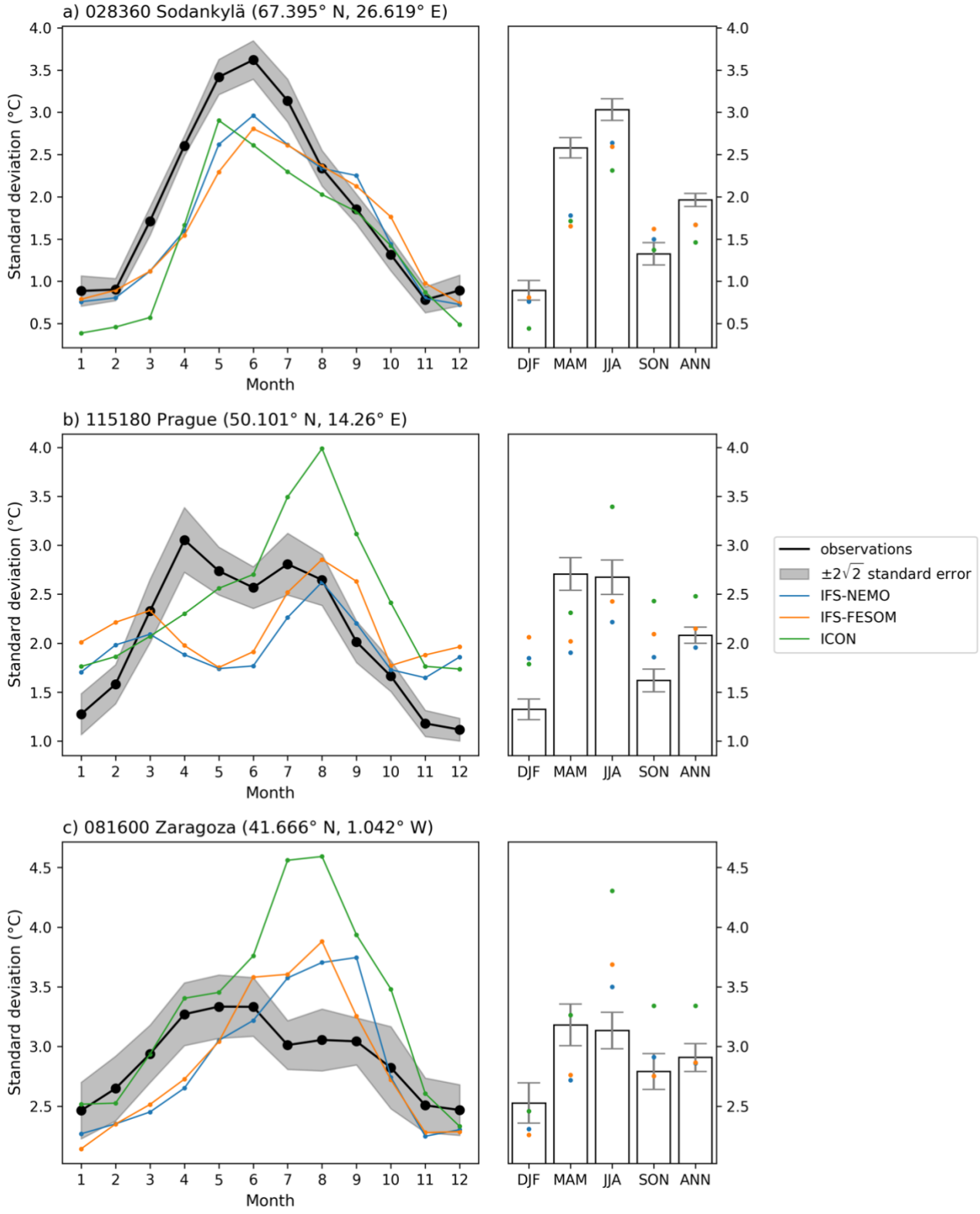

105

Figure S25. As Figure S9, but for the intramonth standard deviation of 2-metre dew point difference (°C).

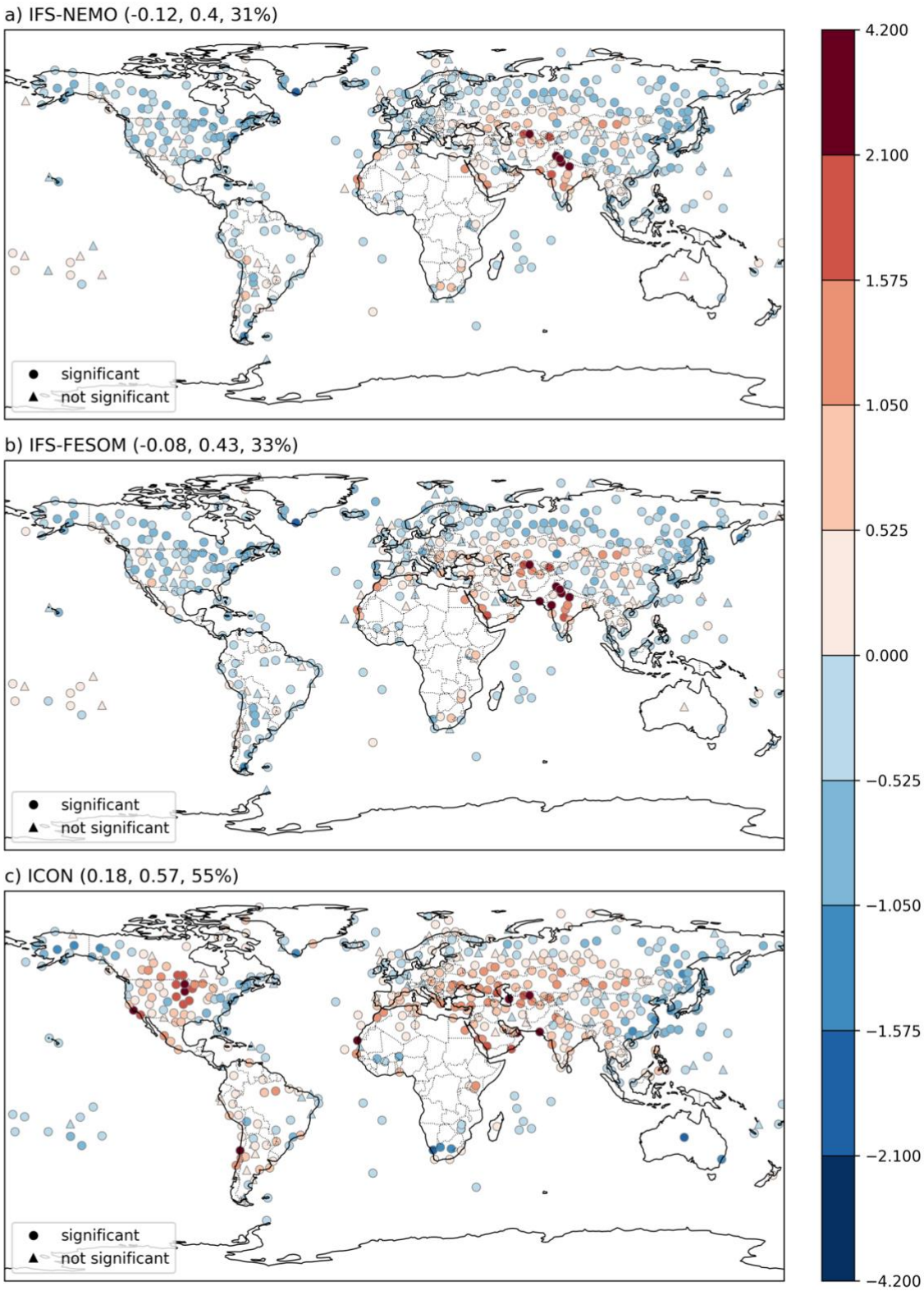

Figure S26. As Figure S10, but for the annually averaged intramonth standard deviation of 2-metre dew point difference (°C).

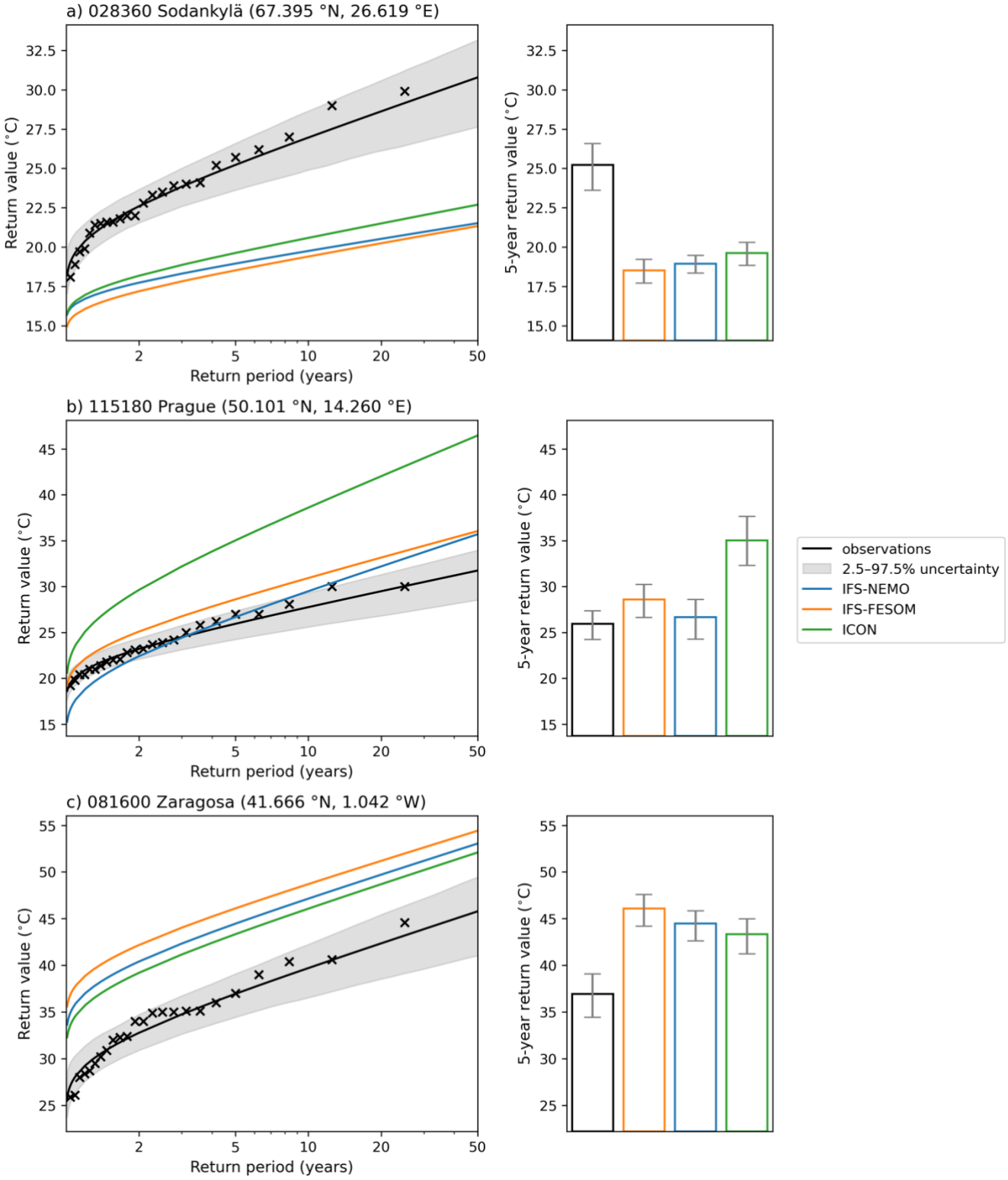

Figure S27. As Figure S11, but for the 5-year return values of the annual maximum 2-metre dew point difference (°C).

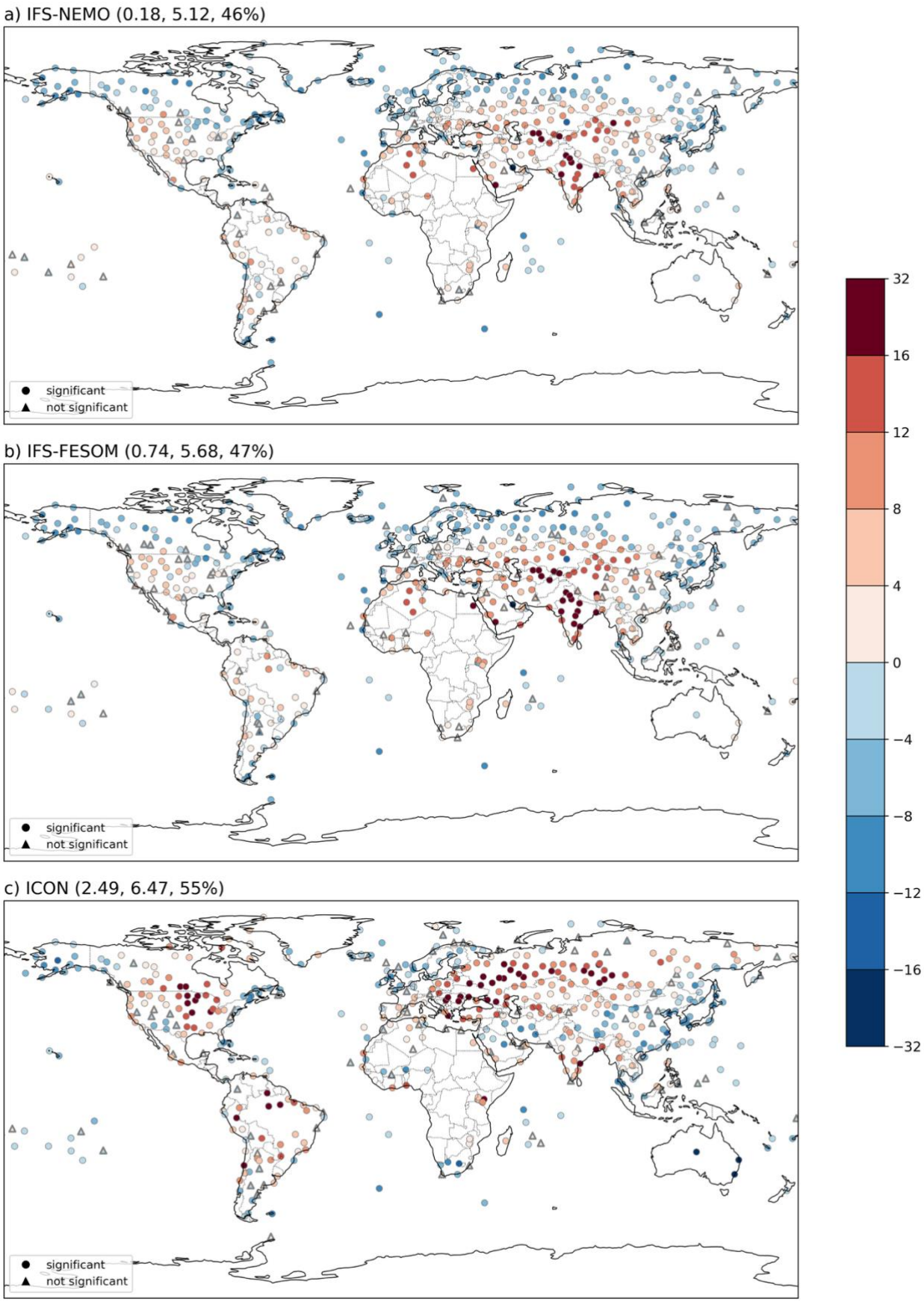

Figure S28. As Figure S12, but for the 5-year return values of annual maximum 2-metre dew point difference (°C).

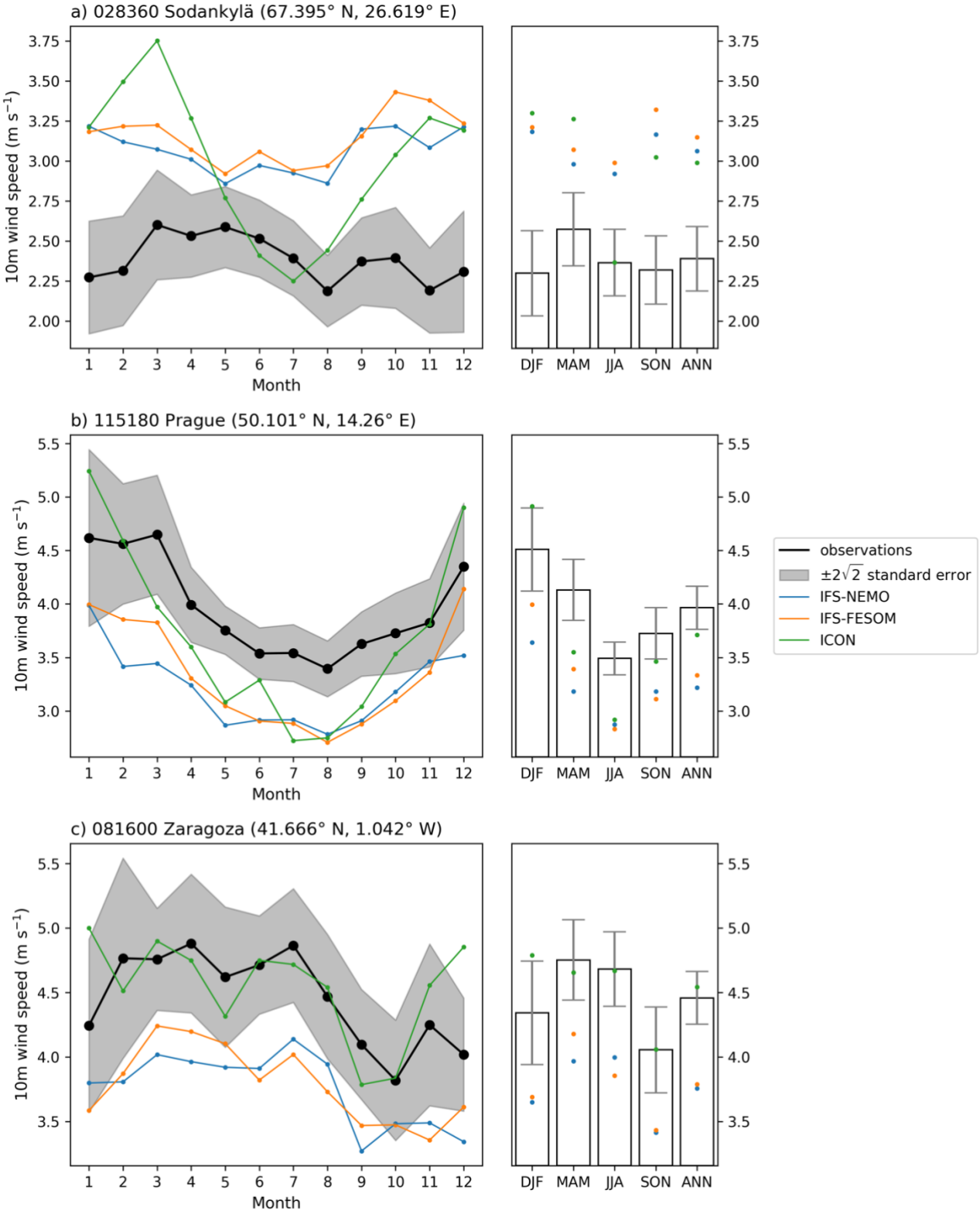

115 **Figure S29**. As Figure S1, but for the mean values of 10-metre wind speed (m s^{-1}).

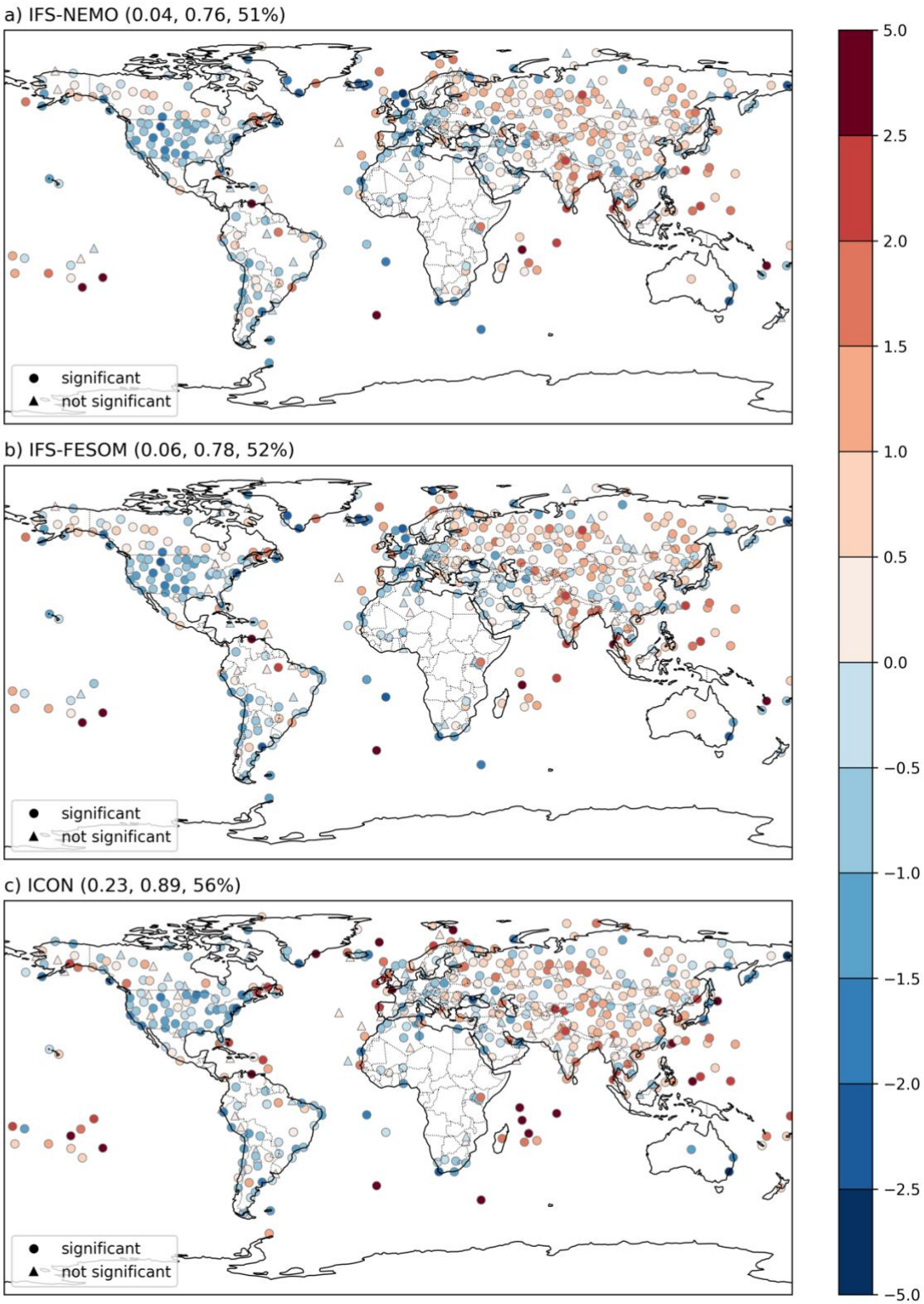

Figure S30. As Figure S2, but for the annual mean bias of 10-metre wind speed (m s^{-1}).

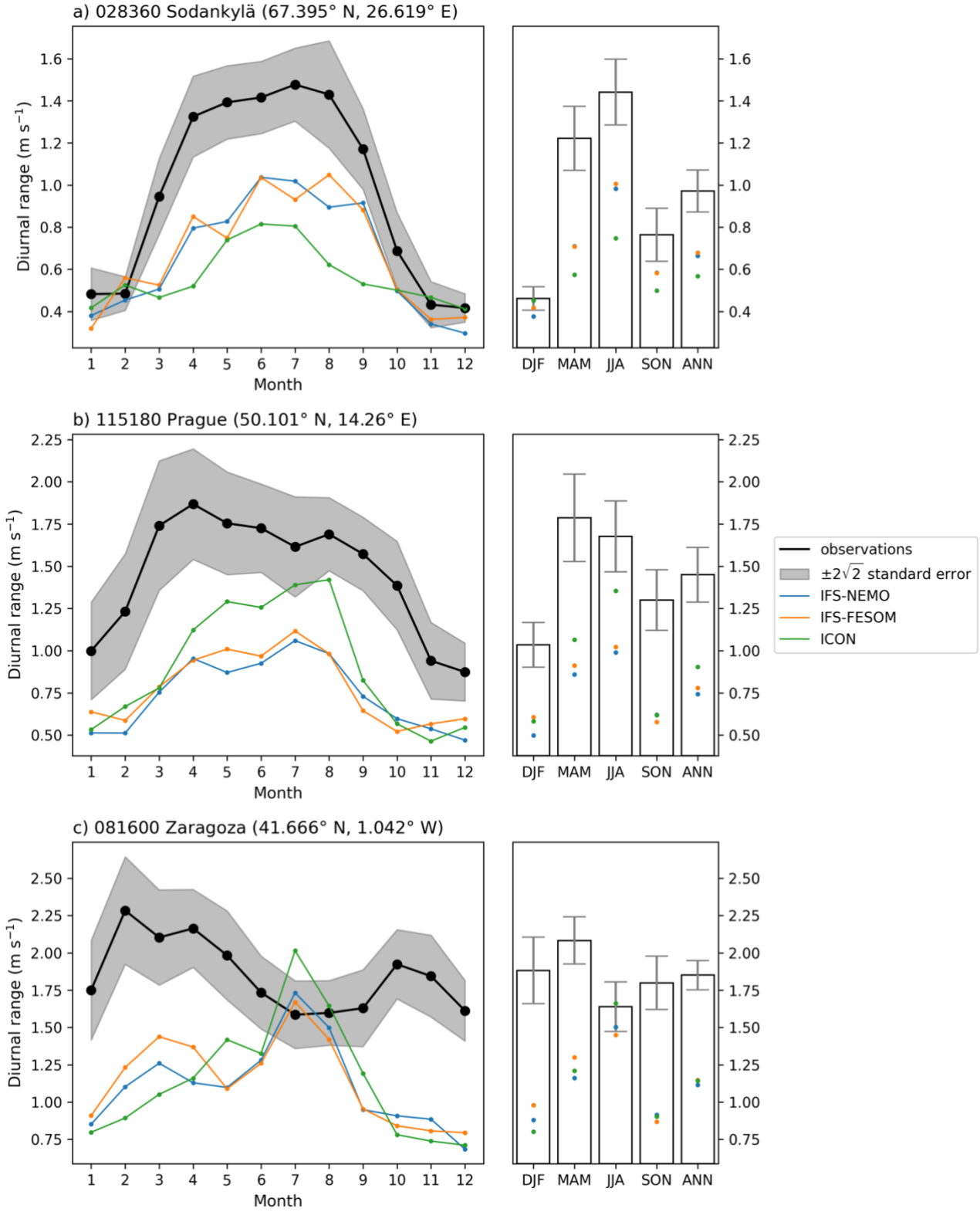

Figure S31. As Figure S3, but for the diurnal range of 10-metre wind speed (m s^{-1}).

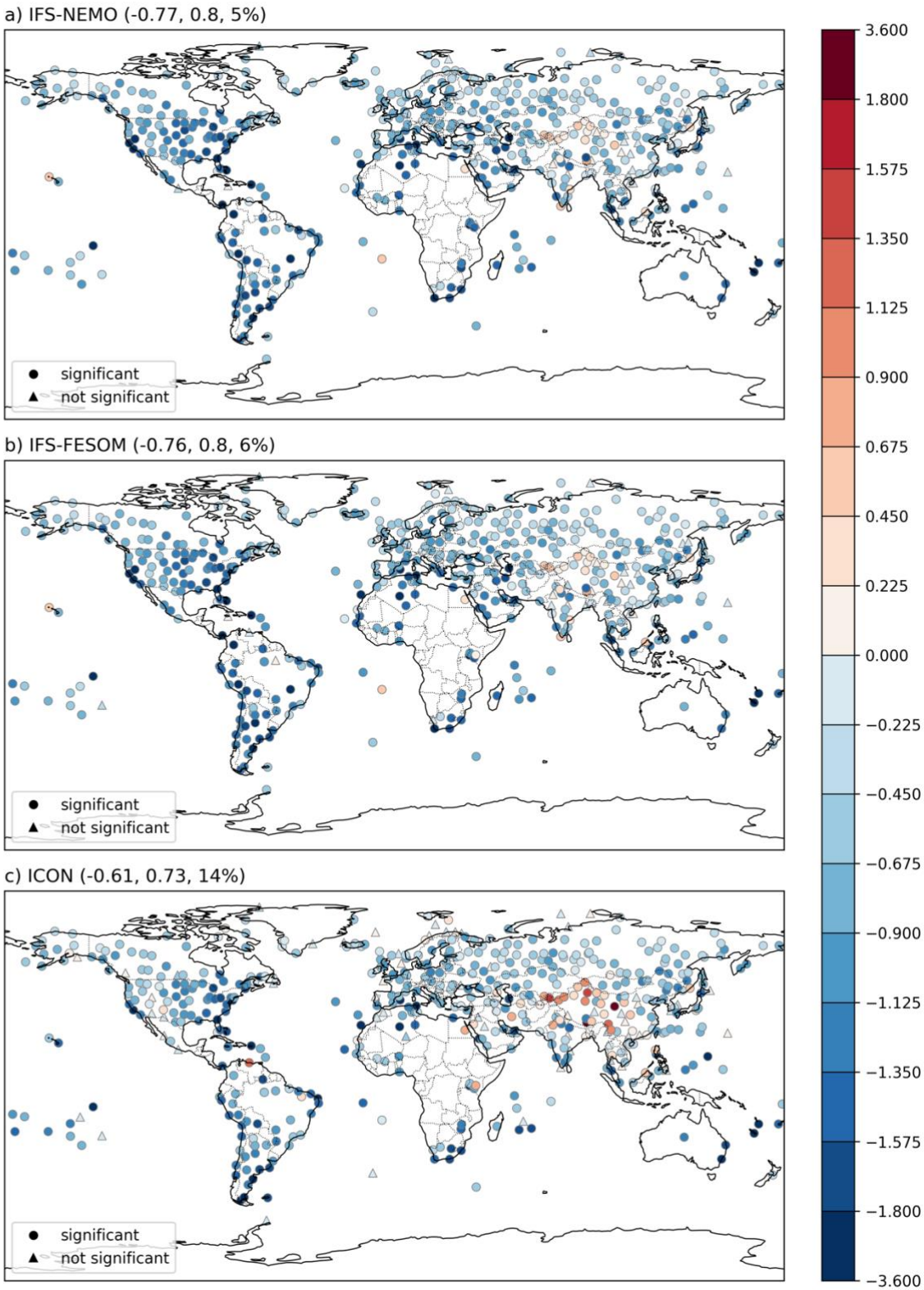

120 **Figure S32**. As Figure S4, but for the annual mean bias in the diurnal range of 10-metre wind speed (m s^{-1}).

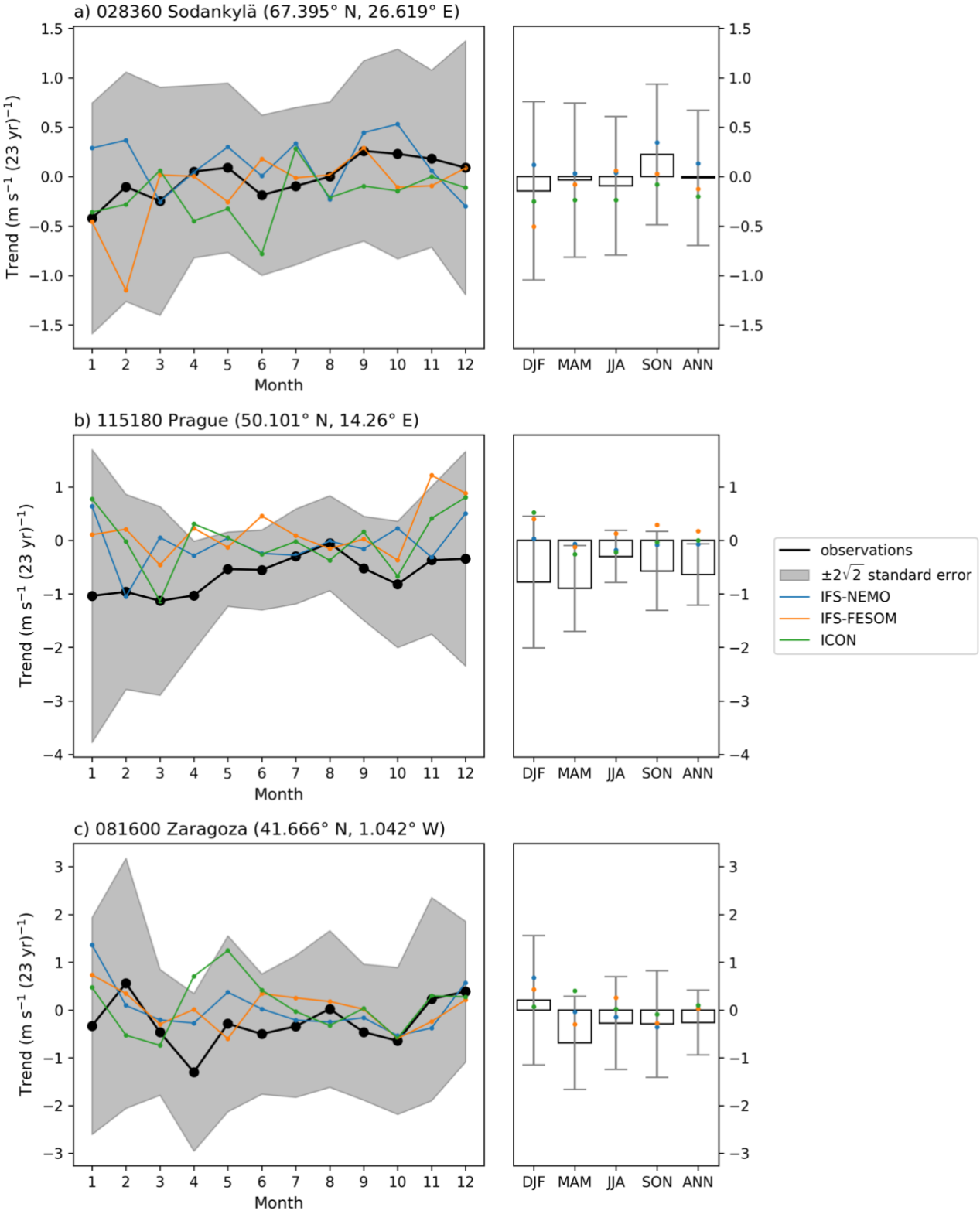

Figure S33. As Figure S5, but for the trend of 10-metre wind speed (m s^{-1} (23 yr^{-1})).

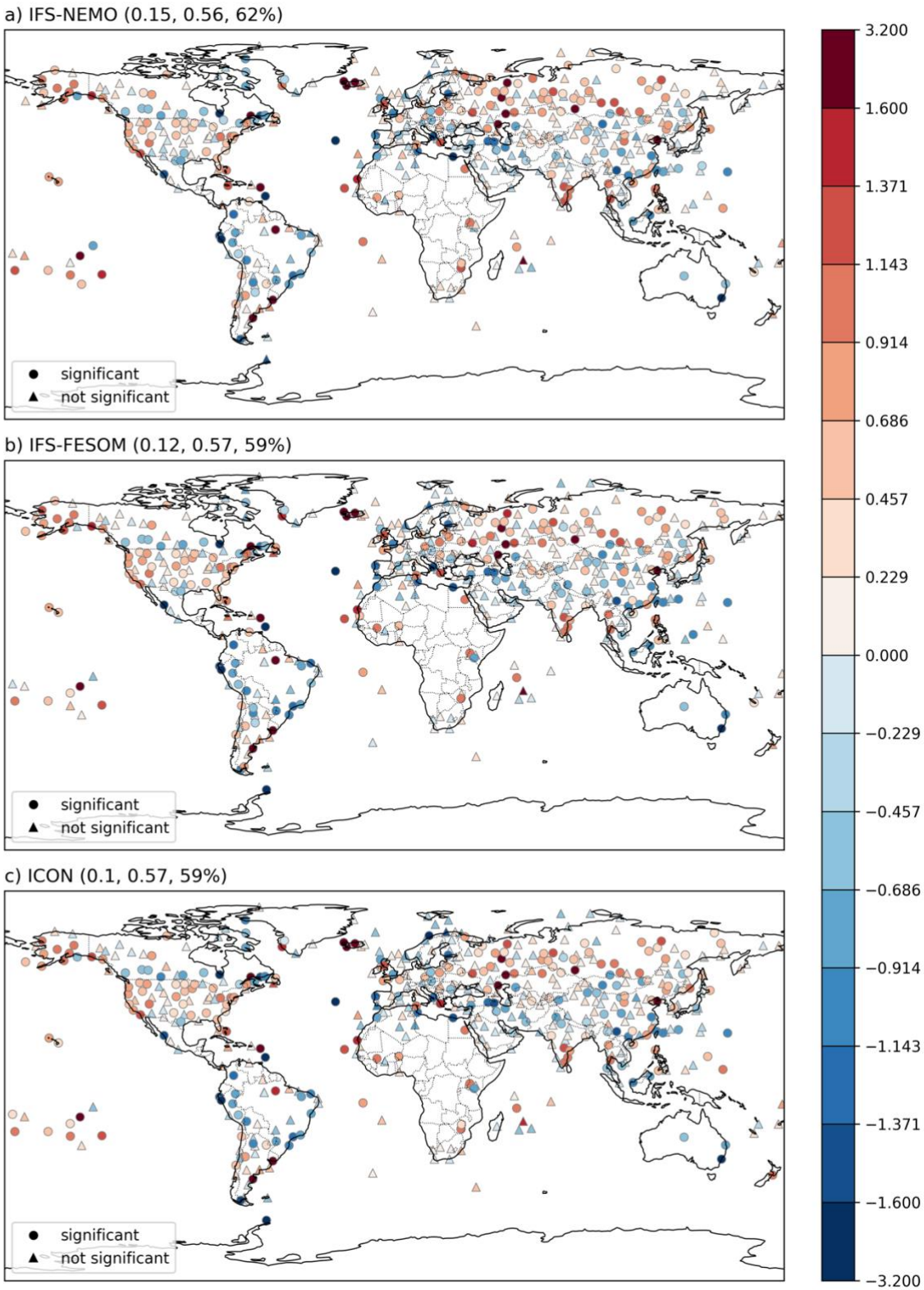

125 **Figure S34**. As Figure S6, but for the linear trend of 10-metre wind speed (m s^{-1} (23 yr^{-1})).

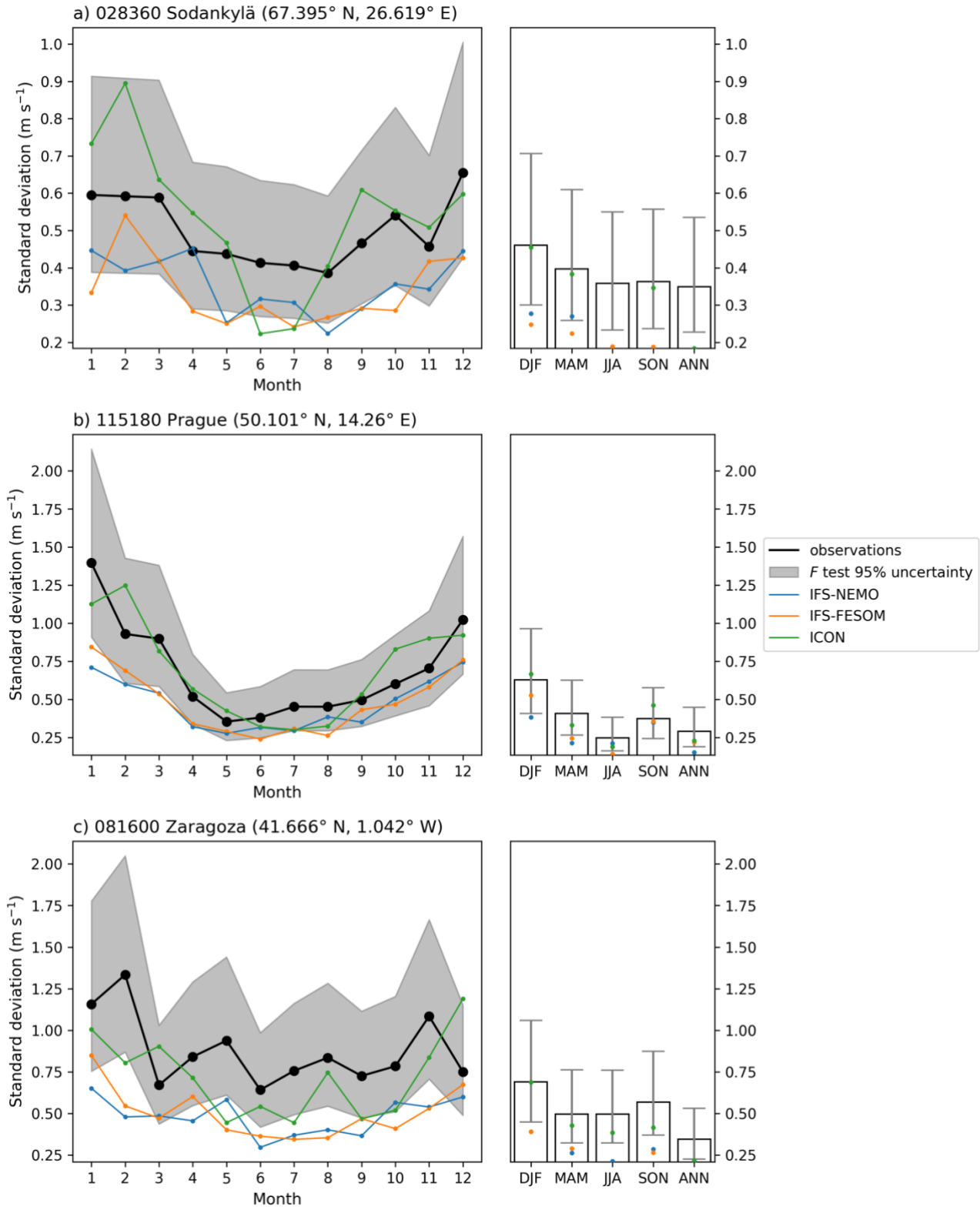

Figure S35. As Figure S7, but for the interannual standard deviation of 10-metre wind speed (m s^{-1}).

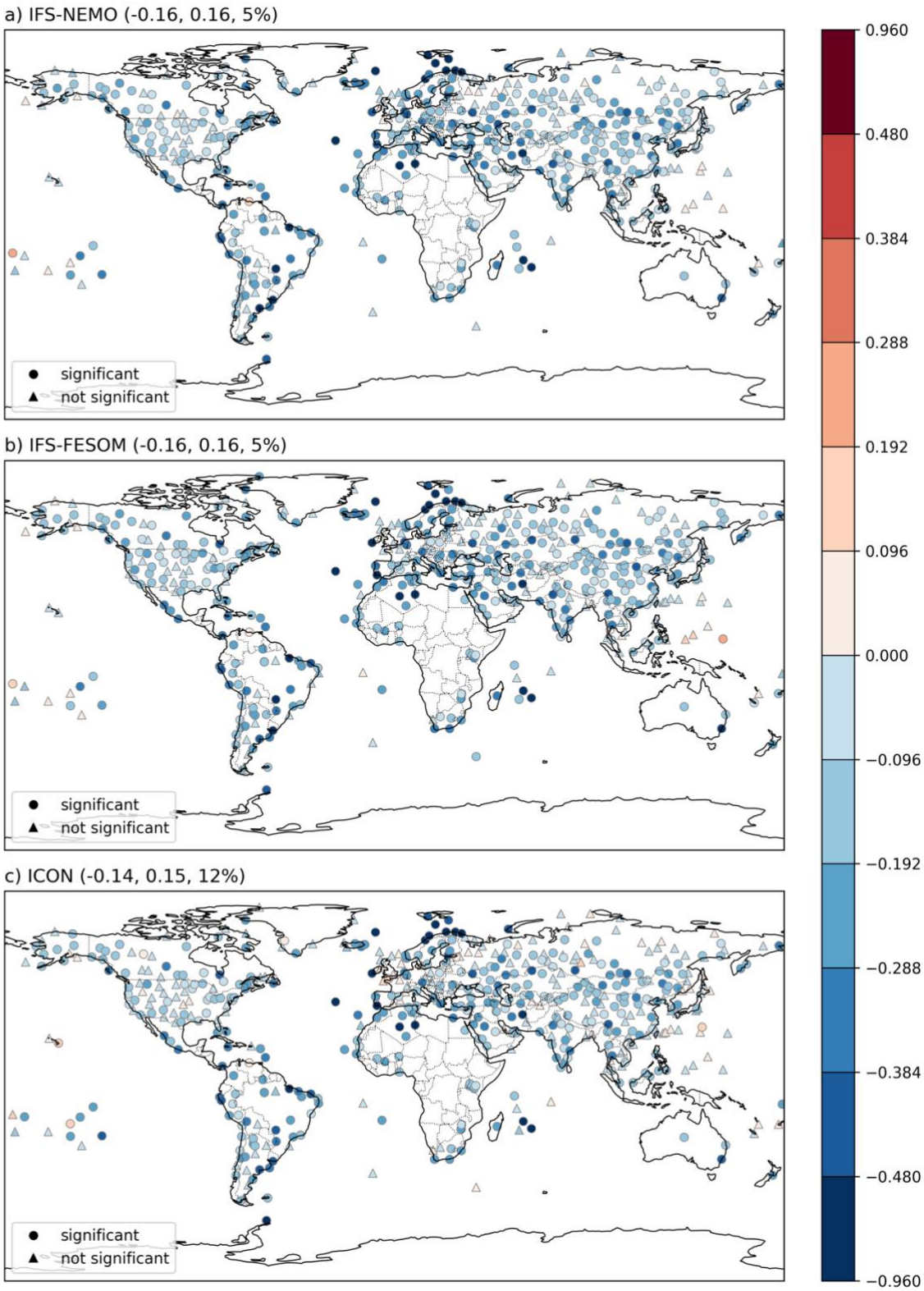

Figure S36. As Figure S8, but for the bias in the interannual standard deviation of annual mean 10-metre wind speed (m s^{-1}).

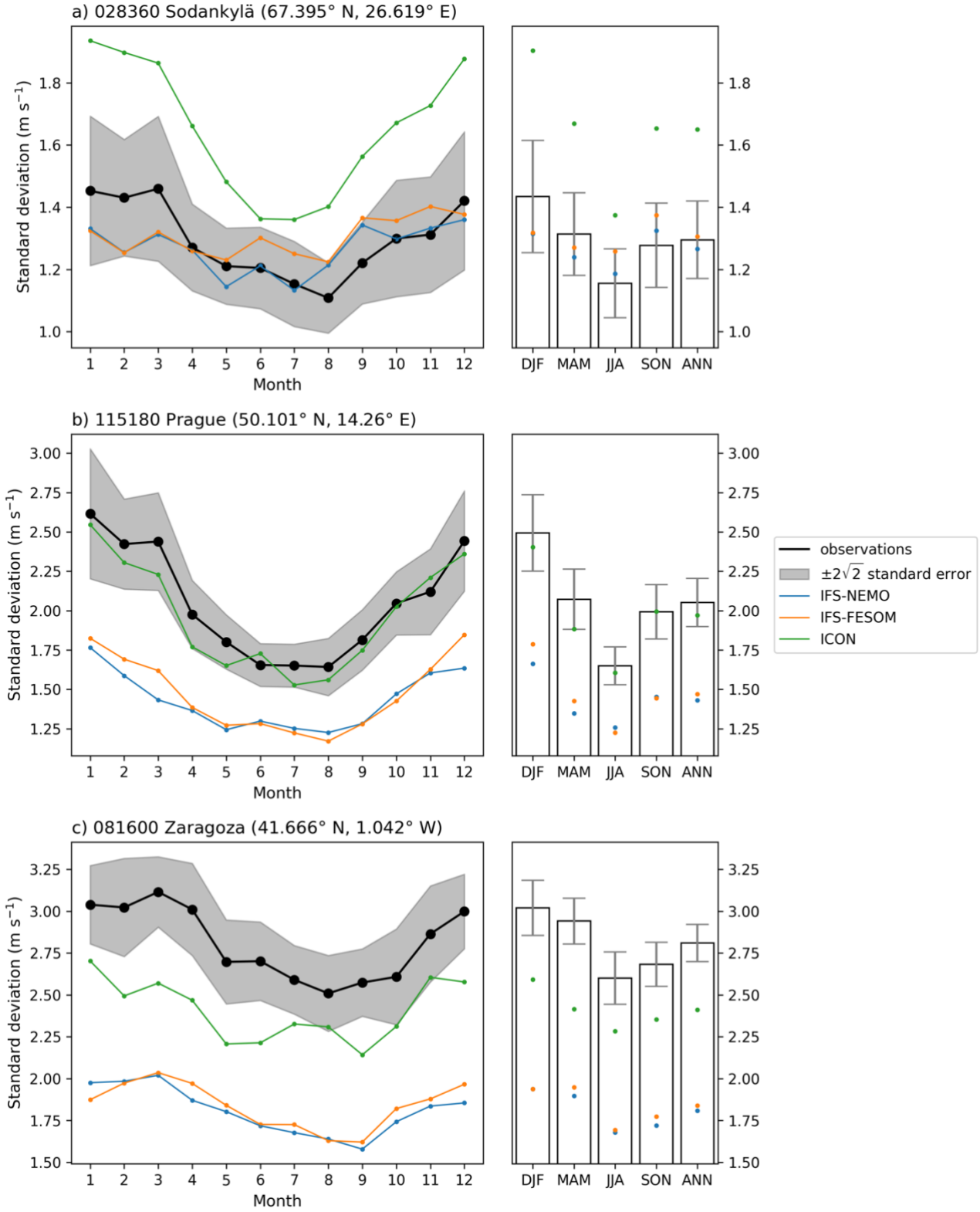

130 **Figure S37**. As Figure S9, but for the intramonth standard deviation of 10-metre wind speed (m s^{-1}).

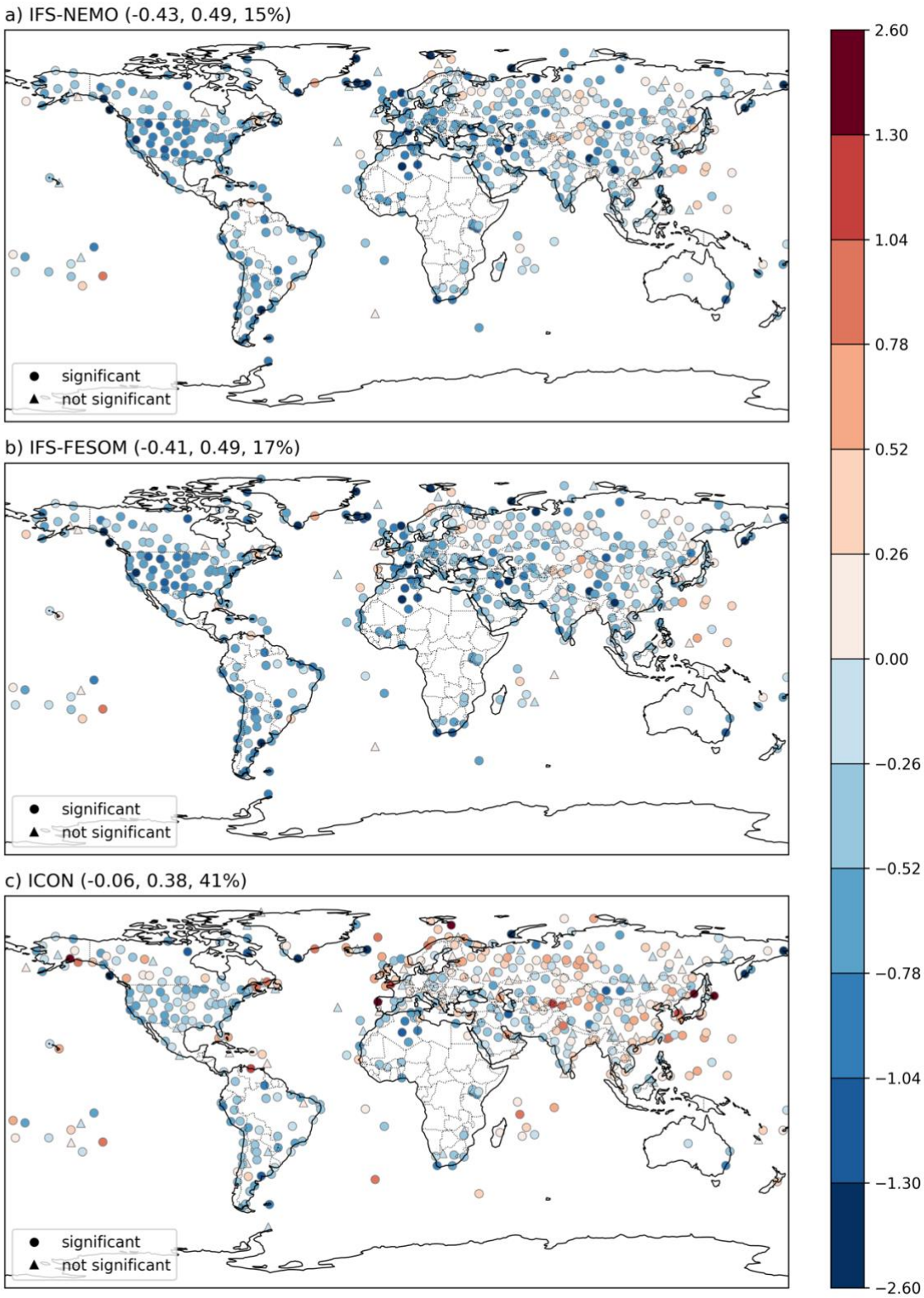

Figure S38. As Figure S8, but for the bias of intramonth standard deviation of annual mean 10-metre wind speed (m s^{-1}).

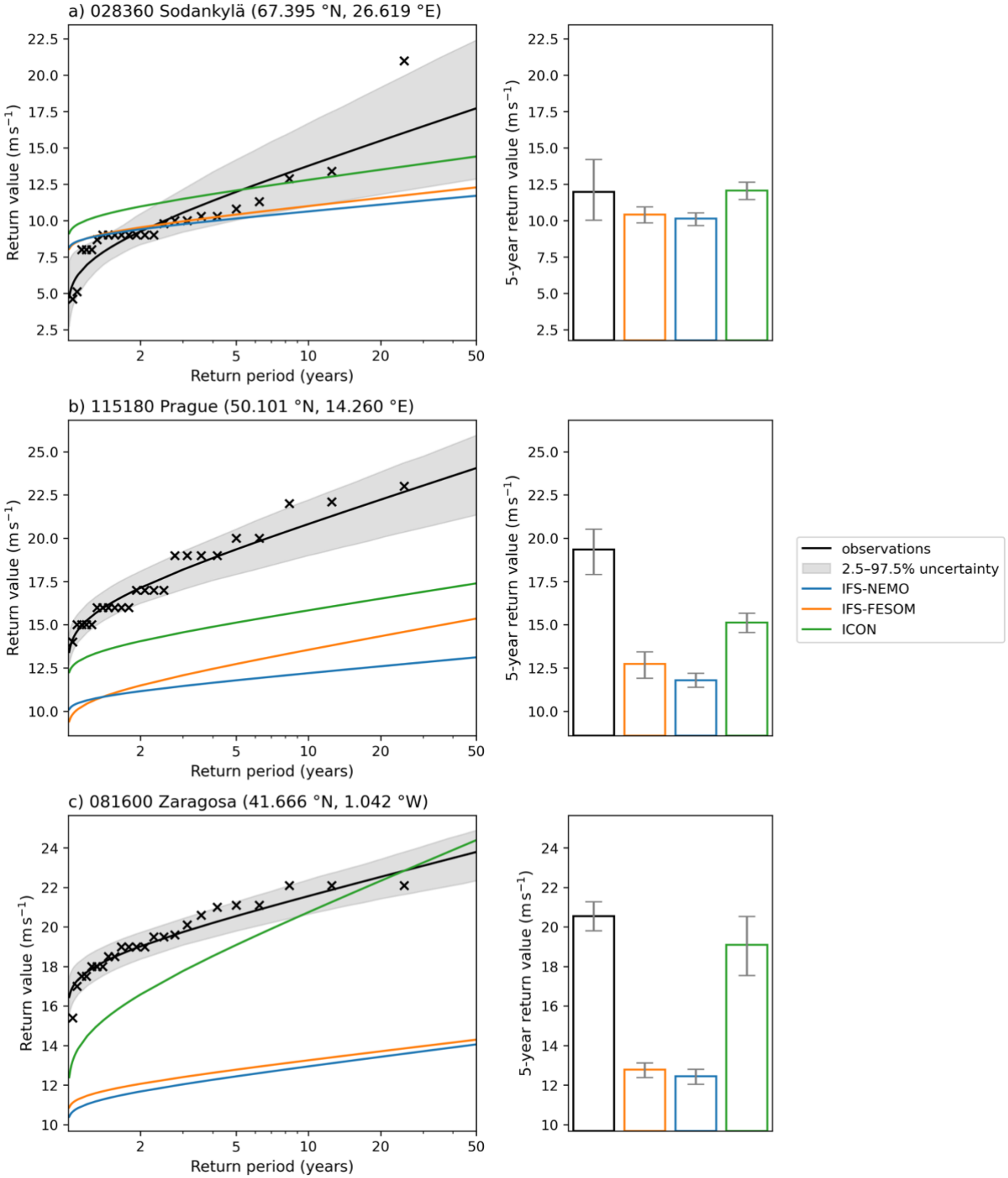

135 **Figure S39**. As Figure S11, but for the 5-year return values of the annual maximum 10-metre wind speed (m s^{-1}).

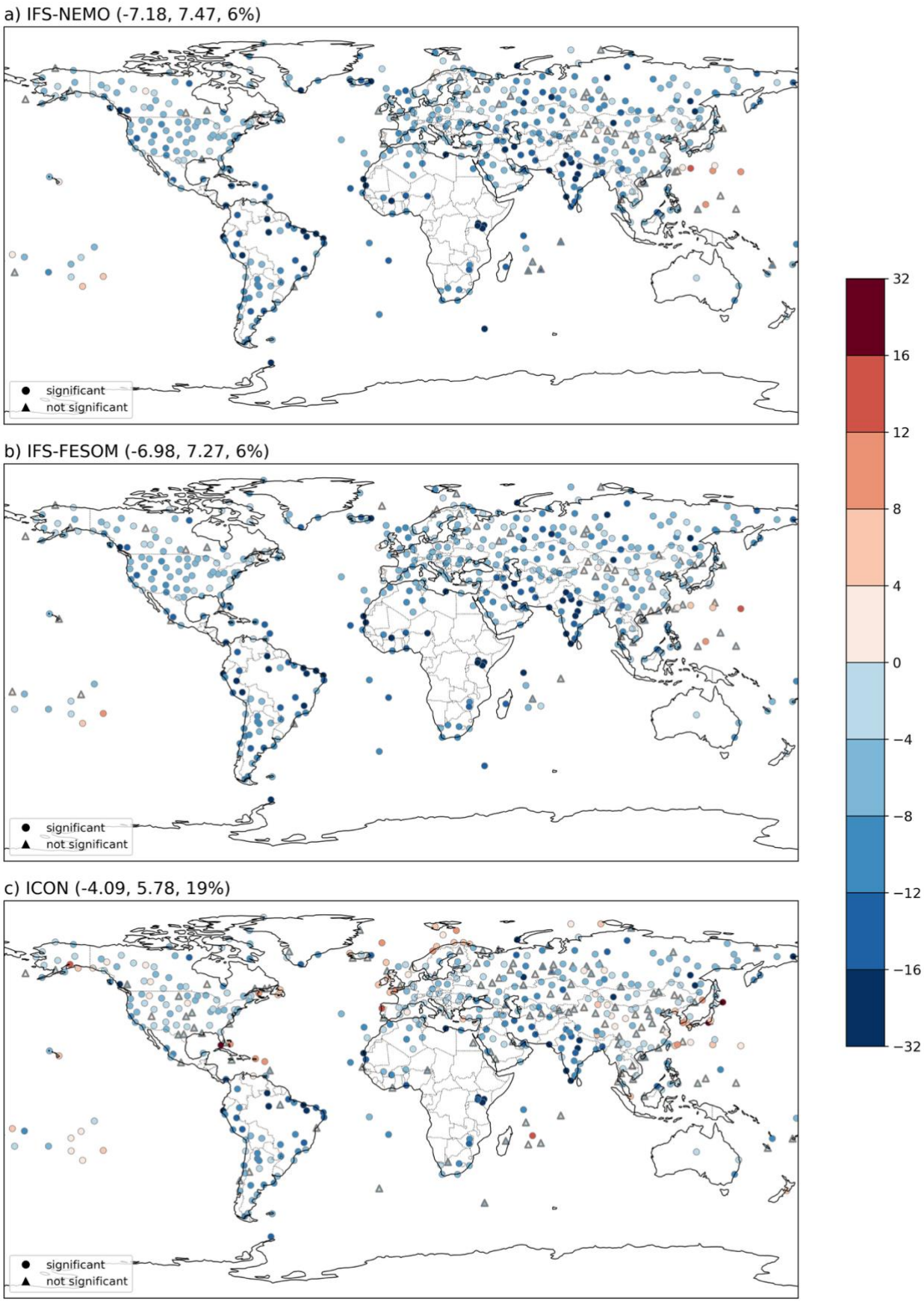

Figure S40. As Figure S12, but for the bias of 5-year return values of the annual maximum 10-metre wind speed (m s^{-1}).